

# On the Considerations of Using Near Real Time Data for Space Weather Hazard Forecasting

A. W. Smith<sup>1</sup>, C. Forsyth<sup>1</sup>, I. J. Rae<sup>2</sup>, T. M. Garton<sup>3</sup>, C. M. Jackman<sup>3</sup>, M. Bakrania<sup>1</sup>, R. M. Shore<sup>4</sup>, G. S. Richardson<sup>5</sup>, C. D. Beggan<sup>5</sup>, M. J. Heyns<sup>6</sup>, J. P. Eastwood<sup>6</sup>, A. W. P. Thomson<sup>5</sup>, J. M. Johnson<sup>7,8</sup>

<sup>1</sup>Mullard Space Science Laboratory, UCL, Dorking, UK

<sup>2</sup>Department of Mathematics, Physics and Electrical Engineering, Northumbria University, Newcastle upon Tyne, UK

<sup>3</sup>School of Cosmic Physics, DIAS Dunsink Observatory, Dublin Institute for Advanced Studies, Dublin 15, Ireland

<sup>4</sup>British Antarctic Survey, Cambridge, UK

<sup>5</sup>British Geological Survey, Edinburgh, UK

<sup>6</sup>Imperial College London, London, UK

<sup>7</sup>Cooperative Institute for Research in Environmental Sciences, University of Colorado Boulder, Boulder, CO, USA

<sup>8</sup>Space Weather Prediction Center, National Oceanic and Atmospheric Administration, Boulder, CO, USA

## Key Points:

- Near-Real-Time solar wind data show increased short-term variability and occasional anomalous values compared to post-processed data.
- Data gaps are most frequently short, meaning short interpolation schemes dramatically increase continuous data availability.
- Data gaps are more prevalent in the plasma moments than the magnetic field from ACE and DSCOVR, but DSCOVR is more continuous.

---

Corresponding author: A. W. Smith, [andy.w.smith@ucl.ac.uk](mailto:andy.w.smith@ucl.ac.uk)

This article has been accepted for publication and undergone full peer review but has not been through the copyediting, typesetting, pagination and proofreading process, which may lead to differences between this version and the [Version of Record](#). Please cite this article as [doi: 10.1029/2022SW003098](https://doi.org/10.1029/2022SW003098).

This article is protected by copyright. All rights reserved.

## Abstract

Space weather represents a severe threat to ground-based infrastructure, satellites and communications. Accurately forecasting when such threats are likely (e.g. when we may see large induced currents) will help to mitigate the societal and financial costs. In recent years computational models have been created that can forecast hazardous intervals, however they generally use post-processed “science” solar wind data from upstream of the Earth. In this work we investigate the quality and continuity of the data that are available in Near-Real-Time (NRT) from the ACE and DSCOVR spacecraft. In general, the data available in NRT corresponds well with post-processed data, however there are three main areas of concern: greater short-term variability in the NRT data, occasional anomalous values and frequent data gaps. Some space weather models are able to compensate for these issues if they are also present in the data used to fit (or train) the model, while others will require extra checks to be implemented in order to produce high quality forecasts. We find that the DSCOVR NRT data are generally more continuous, though they have been available for small fraction of a solar cycle and therefore DSCOVR has experienced a limited range of solar wind conditions. We find that short gaps are the most common, and are most frequently found in the plasma data. To maximize forecast availability we suggest the implementation of limited interpolation if possible, e.g. for gaps of five minutes or less, which could increase the fraction of valid input data considerably.

## Plain Language Summary

The variable plasma conditions in near-Earth space can create hazards for modern society. These include the generation of anomalous ground currents that pose a threat to the operation of infrastructure such as high voltage power grids. Forecasts of intervals when we are likely to be at risk generally use solar wind measurements gathered by satellites from upstream of the Earth. Various computational models have shown skill in predicting risk intervals; however, they are generally created using scientific quality data which are not available in near-real-time (NRT). To prepare for transitioning such models to operational use we assess the similarities and differences between the scientific quality and NRT data. We assess the properties and frequency of data gaps in the NRT data, to build an understanding of how to maximize the time for which forecasts can be successfully created.

## 1 Introduction

Space weather has the potential to pose a severe threat to modern society. The Earth’s magnetosphere is constantly buffeted by the solar wind that emanates from the Sun. It is the variable nature of the solar wind that leads to a highly dynamic environment in near-Earth space. There are many different facets to space weather, including the changing radiation environment in near-Earth space, a hazard that faces Earth orbiting satellites (D. Baker et al., 1987; Iucci et al., 2005), and strong ground magnetic field variability that can induce damaging currents (Geomagnetically Induced Currents, GICs) in conductive infrastructure (Boteler et al., 1998; Boteler, 2021; Rajput et al., 2020). Forecasting intervals of risk in a timely manner is key; this allows necessary mitigating action to be taken.

Space weather forecasts are typically driven by data obtained upstream of the Earth at the L1 point (e.g. D. N. Baker et al., 1990; Wing et al., 2005; Forsyth et al., 2020; Keesee et al., 2020; A. W. Smith, Forsyth, Rae, Garton, et al., 2021; Chu et al., 2021), approximately 1.5 million km ahead of the Earth. Given the speed of the solar wind, this provides between 20 - 90 minutes of warning before solar wind plasma encounters the Earth (Baumann & McCloskey, 2021). To account for the variable time delay between the plasma measured at L1 and the arrival of that plasma at the Earth, many forecast models propagate the measurement to a fixed point relative to the Earth, the bow shock for exam-

75 ple (e.g. Cash et al., 2016; Baumann & McCloskey, 2021). Such methods are present in  
76 commonly used scientific datasets, such as the OMNI database (<https://omniweb.gsfc.nasa.gov/>)  
77 (Weimer & King, 2008), and will have implications for data continuity.

78 Further, most current space weather forecasting models have been developed using  
79 post-processed, scientific quality data provided by the spacecraft at L1, or combined  
80 data products such as OMNI (e.g. Wintoft et al., 2017; Keesee et al., 2020; A. W. Smith,  
81 Forsyth, Rae, Garton, et al., 2021). Such data are generally only available after an extended  
82 period, beyond the interval in which a timely forecast must be made. Data are  
83 also available in near-real time (NRT), usually within five minutes of acquisition by the  
84 spacecraft (e.g. Zwickl et al., 1998). However, given limited telemetry and processing  
85 the NRT data are an approximation of the full scientific data that will later be available.  
86 This may lead to differences in the value that the data take, and also whether data are  
87 available for some intervals (e.g. Machol et al., 2013). Nonetheless, the NRT data must  
88 be used in order to provide actionable forecasts of upcoming hazardous space weather.

89 In this work we explore how we may best use the data available in NRT to produce  
90 space weather forecasts. We will use the example of the space weather threat to ground  
91 based infrastructure through GICs. GICs pose a severe threat to continuous and reliable  
92 power network operation in many countries around the world (e.g. Gaunt & Coetsee,  
93 2007; Marshall et al., 2012), particularly at higher latitude locations (e.g. Bolduc,  
94 2002). Even at mid-latitude locations, such as the UK, the estimated cost of a major geomagnetic  
95 storm - one that leads to a widespread and long-lasting interruption of electrical supply -  
96 has been estimated at billions of dollars a day (Oughton et al., 2017). However, with  
97 sufficient warning mitigating actions may be taken that would reduce this cost  
98 considerably (Eastwood et al., 2018; Oughton et al., 2019). Therefore, the forecasting  
99 and mitigation of large, damaging GICs is a critical endeavour.

100 GICs are driven by magnetic field variability at Earth's surface as a consequence  
101 of Faraday's law of induction. Though mainly discussed with respect to power networks  
102 (e.g. Pulkkinen et al., 2005; Mac Manus et al., 2017; Divett et al., 2018; Rajput et al.,  
103 2020), GICs may be induced in any large scale conducting infrastructure, such as pipelines  
104 (e.g. Campbell, 1980; Gummow & Eng, 2002; Viljanen et al., 2010; Dimmock et al., 2021)  
105 and railways (e.g. Wik et al., 2009; Liu et al., 2016; Love et al., 2019), with consequences  
106 ranging from increased corrosion to direct component failure. Ultimately strong magnetic  
107 field variability is driven by a myriad of magnetospheric processes in near-Earth  
108 space (e.g. Heyns et al., 2021; Rogers et al., 2020; Tsurutani & Hajra, 2021). Extreme  
109 field fluctuations are often linked to global scale transient phenomena such as geomagnetic  
110 storms (Kappenman & Albertson, 1990; Dimmock et al., 2019), substorms (Viljanen  
111 et al., 2006; Turnbull et al., 2009; Freeman et al., 2019) and sudden commencements (Rodger  
112 et al., 2017; A. W. Smith et al., 2019; A. W. Smith, Forsyth, Rae, Rodger, & Freeman,  
113 2021).

114 Work in recent years has explored both empirical and first-principles methods to  
115 forecast the surface geomagnetic field or geomagnetic perturbations. These methods have  
116 included statistical techniques (e.g. Weigel et al., 2002; Weimer, 2013; Shore et al., 2017),  
117 global scale physics-based (Magneto-HydroDynamic, MHD) models (e.g. Pulkkinen et  
118 al., 2011, 2013; Tóth et al., 2014; Welling, 2019), machine learning-based techniques (e.g.  
119 Gleisner & Lundstedt, 2001; Wintoft et al., 2015, 2017; Keesee et al., 2020; A. W. Smith,  
120 Forsyth, Rae, Garton, et al., 2021; Blandin et al., 2022; Pinto et al., 2022; Upendran et  
121 al., 2022), or combinations of these methods (e.g. Camporeale et al., 2020). The forecast  
122 geomagnetic (or geoelectric) field predictions can then be used to drive models based  
123 on the local geology and properties of the power network to indirectly obtain GIC estimates  
124 (Beggan et al., 2013; Blake et al., 2016, 2018; Divett et al., 2018, 2020; Dimmock  
125 et al., 2021; Grawe & Makela, 2021; Mac Manus et al., 2022). Each model that is used  
126 to forecast the geomagnetic consequences of space weather will use the input solar wind

127 data in a distinct fashion, and therefore may be impacted differently by the ways in which  
 128 the NRT and scientific data differ.

129 In this study we explore the data that are available from the L1 point in NRT and  
 130 investigate how they may be used by space weather forecasting models. In Section 2 we  
 131 describe the data, while in Section 3 we evaluate the NRT data, including comparisons  
 132 to the more commonly used scientific quality data. In Section 4 we show the results of  
 133 training an example forecasting model on the NRT data, using a model based on A. W. Smith,  
 134 Forsyth, Rae, Garton, et al. (2021). Section 5 then discusses the results in the context  
 135 of producing space weather forecasts in near real time.

## 136 2 Data

137 In this study we use and explore the data made available by SWPC (the Space Weather  
 138 Prediction Center) in near real time (NRT) from the ACE (Advanced Composition Ex-  
 139 plorer) and DSCOVR (Deep Space Climate Observatory) satellites located at L1. ACE  
 140 launched in 1997 as a part of the NASA Explorer program and has provided solar wind  
 141 observations since 1998 (Stone et al., 1998). Meanwhile, DSCOVR was a NASA/NOAA  
 142 mission that launched more recently in 2015. The NRT data is provided at one minute  
 143 resolution (Zwickl et al., 1998). For the magnetic field we consider the three GSM (Geo-  
 144 centric Solar Magnetospheric) components of the magnetic field ( $B_X^{GSM}$ ,  $B_Y^{GSM}$ ,  $B_Z^{GSM}$ )  
 145 and the total field strength ( $|B|$ ) (C. Smith et al., 1998). Meanwhile, for the plasma data  
 146 we evaluate the derived proton density ( $n_p$ ), solar wind bulk speed ( $V$ ) and ion temper-  
 147 ature ( $T_i$ ) (McComas et al., 1998; Aellig et al., 2001).

148 The ACE spacecraft was the operational real time solar wind monitor at L1 un-  
 149 til mid-2017, at which time it was replaced by DSCOVR. In this study we therefore use  
 150 data from ACE between 1999 and 2015 (inclusive) and from DSCOVR between 2018 and  
 151 2020 (inclusive). This selection ensures we are using intervals in which each spacecraft  
 152 was the primary real time operational solar wind monitor, and therefore prioritized for  
 153 telemetry downlink. We note that even though DSCOVR is currently the operational  
 154 real time solar wind monitor, data from ACE may occasionally be used to fill large miss-  
 155 ing intervals in the DSCOVR data. Due to issues with the spacecraft, DSCOVR data  
 156 are largely absent between 06/26/19 and 02/26/20, however we do not perform any sub-  
 157 stitution with ACE during this period, and simply use the data that are available. Switch-  
 158 ing the data between spacecraft that are not co-located or cross-calibrated results in its  
 159 own challenges that are beyond the scope of this work.

160 In Sections 3 and 4 we use scientific quality data for comparative purposes. For ACE  
 161 we use H0 data (level 2), that have been re-sampled to the same one minute cadence as  
 162 the NRT data. For the magnetic field data this means they are down sampled from a  
 163 16s cadence, while the plasma moments are up sampled from a 64s cadence. We note  
 164 that if we instead down sampled the NRT measurements to 64s prior to running the anal-  
 165 ysis it would result in very small changes ( $\leq 0.4\%$ ) to the quantitative comparisons per-  
 166 formed. Meanwhile, for DSCOVR we use H0 magnetic field data (down-sampled from  
 167 1s resolution), and H1 plasma moments at a one minute resolution. The DSCOVR H1  
 168 plasma moments are currently only available until 06/27/2019, limiting the time inter-  
 169 val for which the comparison with the NRT data can be evaluated.

## 170 3 Data Evaluation

171 The NRT data from the DSCOVR and ACE spacecraft at L1 are available within  
 172 minutes of recording by the spacecraft and are therefore automatically processed. On  
 173 the ground further processing steps, such as manual data review, data cleansing, more  
 174 complex fitting methods and recalibration are used to produce science quality data. It  
 175 is important to consider any differences between these two types of data when moving

space weather models from the science quality data on which they were likely developed/evaluated to the operational NRT data. Though DSCOVR is the current operational solar wind monitor some models require large quantities of training data and thus the historical ACE NRT data are also of interest. Below, we evaluate the NRT data values for ACE and DSCOVR, as well as their continuity.

### 3.1 Data Validity

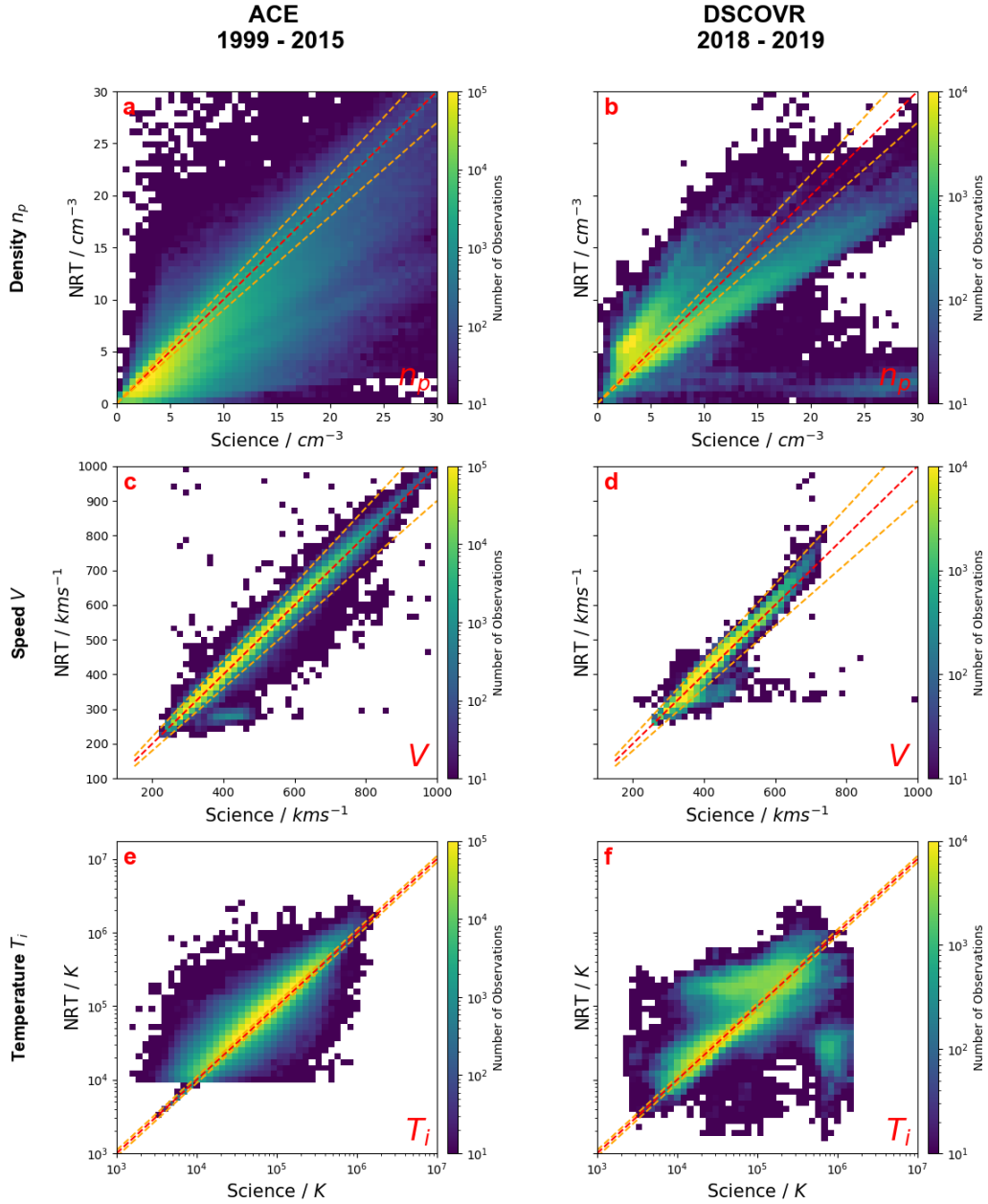
First, we compare the values returned by the NRT data and the equivalent science quality data that is released later after post-processing. Figure 1 shows a series of two-dimensional histograms of the occurrence of plasma moment values in these data sets for ACE (left) and DSCOVR (right). We note that if either data set (NRT or science) is missing then that interval is not represented in Figure 1. Additionally, in this analysis our base assumption is that the science data are the “correct” values, to which the NRT data represent an initial estimate. Therefore, in an ideal situation we would observe the case where both the science and NRT values are close, and lie along the red dashed lines (or the NRT data are within  $\pm 10\%$  of the scientific values). However, we see deviations from this for both the ACE and DSCOVR data.

Inspecting the results for the ACE data (left of Figure 1) we see that the plasma velocity is best represented in the NRT data (Figure 1c), with the histogram most closely following the diagonal line of equality and the vast majority of the data (96%) being bounded by the orange  $\pm 10\%$  lines. In contrast, the solar wind density (Figure 1a) and ion temperature (Figure 1e) are less well captured by the ACE NRT data, showing much larger spreads: only  $\sim 20\text{--}30\%$  of both NRT data sets are within 10% of the science values. We also see evidence for a hard-coded lower limit to the NRT ion temperatures (Figure 1e).

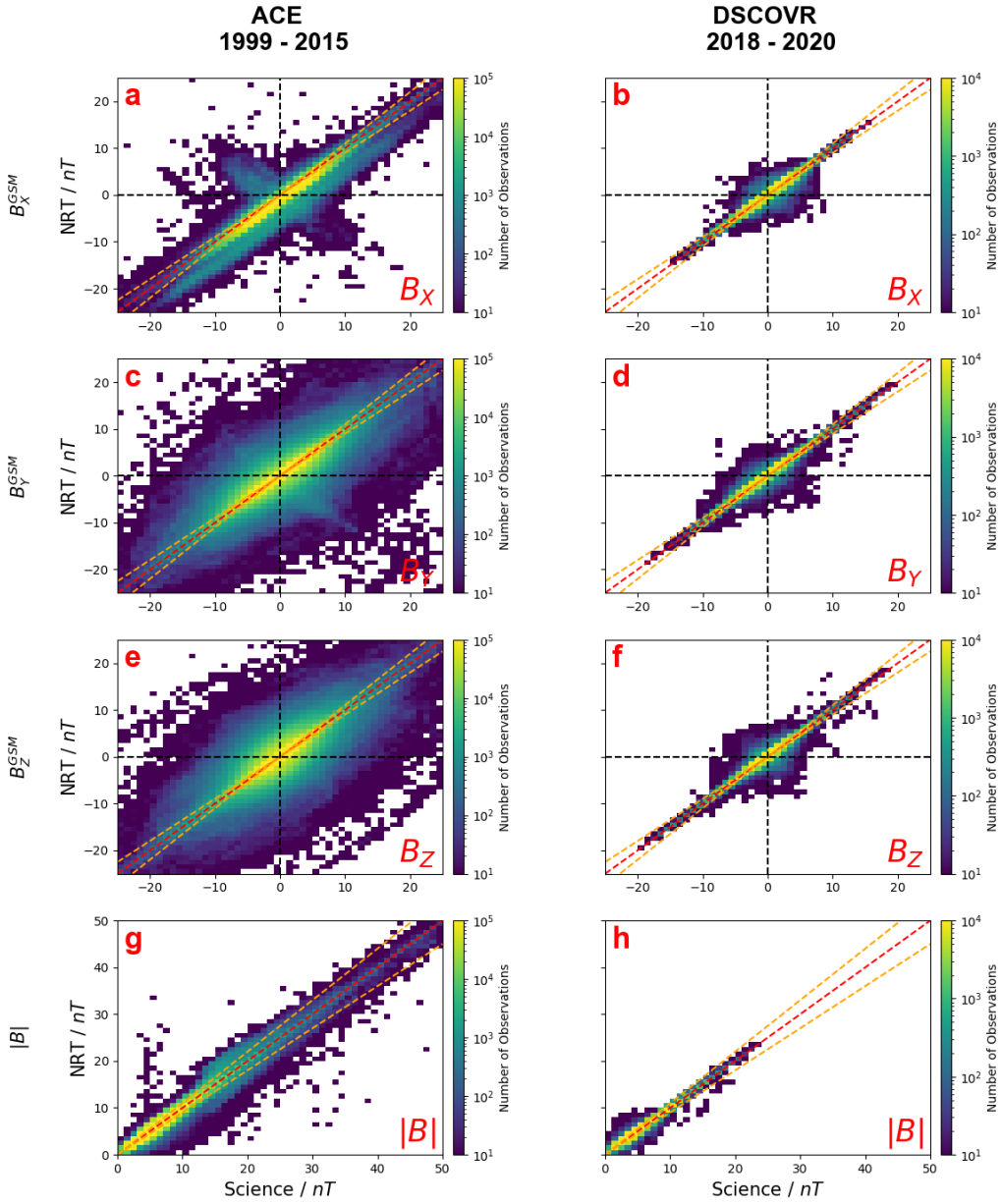
Considering the DSCOVR data (right of Figure 1), we once again find that the plasma velocity is best captured by the NRT data (Figure 1d). The vast majority of the DSCOVR data lie along the red dashed line, with 94% of the NRT data within 10% of the science values. We find similar spread in the DSCOVR density comparison (Figure 1b) as we did for the ACE data ( $\sim 20\%$  within  $\pm 10\%$ ). NRT data from both spacecraft appear to commonly underestimate the plasma density. Finally, considering the NRT temperatures reported by DSCOVR we find 20% of the data within the  $\pm 10\%$  lines, slightly less than the 30% found for the ACE data. We note that the DSCOVR spacecraft has been operational for a shorter interval, and so has experienced fewer extreme events (e.g. at larger  $n_p$  or  $V$ ).

Figure 2 shows a similar comparison of the magnetic field data, comparing the NRT and science data for ACE (left) and DSCOVR (right). Statistically, the ACE data are peaked around the diagonal line of gradient unity, though there is wide spread in values. This suggests that the magnetic field values are often corrected later on, sometimes by 10s of nT. There is noticeably less spread in the comparison of the  $B_X^{GSM}$  values (Figure 2a), though interestingly there are a series of values that seem to form a parallel distribution to the red line. This would correspond to a small offset of 5 nT or less, where the NRT data under-reported the value of  $B_X^{GSM}$ . There is also evidence of a distribution perpendicular to the line of equality in the results for  $B_X^{GSM}$  and  $B_Y^{GSM}$ , perhaps representing a rotation of the magnetic field in the X-Y plane. We note that despite the spread in the field components reported by ACE, 68% of the NRT measurements of the total field magnitude ( $|B|$ ) are within  $\pm 10\%$  of the science values.

When we compare the DSCOVR results (right of Figure 2), we again find that the NRT data are much more representative of the science data than was observed for ACE, with a clear diagonal distribution dominating the results. As with ACE, the NRT total field strength ( $|B|$ ) is also very close to that later found within the science data, with 94% of the values being within 10%.



**Figure 1.** Comparison of the plasma moments in the NRT data with that recovered in the science quality data. Left column (a, c, e) shows ACE between 1999 and 2015 (inclusive), right column (b, d, f) shows DSCOVR between 2018 and mid-2019. The plasma moments shown are the plasma density (a, b), bulk velocity (c, d), and ion temperature (e, f). The diagonal red dashed line indicates where the data returned are equivalent, while the orange dashed lines indicate the region where the NRT values are within  $\pm 10\%$  of the science data.



**Figure 2.** Comparison of the magnetic field values returned by the NRT data and science data. The format is similar to Figure 1, with the ACE (1999 to 2015) shown on the left (a, c, e, g) and DSCOVR (2018 to 2020) on the right (b, d, f, h). The top row shows the  $B_X^{GSM}$  component (a, b), the second row shows the  $B_Y^{GSM}$  (c, d), while the third and fourth rows show the  $B_Z^{GSM}$  (e, f) and total field  $|B|$  (g, h).

227

### 3.2 Data Continuity

228

229

230

231

232

233

234

235

236

237

238

239

The magnetosphere is a highly dynamic system that couples to the solar wind on a range of time scales (e.g. Coxon et al., 2019; Shore et al., 2019; Borovsky, 2020). Space weather models therefore often require information regarding the preceding interval of solar wind, rather than a single measurement of the current conditions. Incomplete data - those with communication gaps or missing measurements - may pose a problem for this approach. Data gaps have also been inferred to cause errors in the derivation of coupling functions (Lockwood et al., 2019). There are many reasons why data may be missing from the real time data stream, or should be ignored. Missing data are generally flagged with a code according to the reason, be it an operational consideration (e.g. downlink issues) or problems/failure of the measurement or recording. It may be possible to develop bespoke solutions to account for different missing data flags, however in the following we treat all missing and/or flagged data identically.

240

#### 3.2.1 Data Gap Occurrence

241

242

243

244

245

246

247

248

249

250

251

252

253

Figure 3 demonstrates the average yearly occurrence of data gaps with different lengths in the NRT data from ACE (top) and DSCOVR (bottom). The equivalent distributions for the science data sets are shown in black. Starting with ACE, we can see that the most common data gap length in both data sets is five minutes or less, i.e. five or fewer data points. We observe that there are nearly 200,000 gaps per year of less than five minutes in the plasma data (Figure 3b). The ACE NRT magnetic field data is more complete by comparison, and whilst the sub-five-minute data gaps are the most common type, there are only around 4000 of these per year. Comparing the scientific and NRT data, we see that the ACE scientific magnetic field data is much more continuous, with several orders of magnitude fewer gaps per year (of any duration). Meanwhile, for the ACE plasma data we see that there are generally fewer gaps shorter than  $\sim 60$  minutes in the science data, but there are on average more gaps of greater duration, perhaps as longer windows of data are later flagged for removal.

254

255

256

257

258

259

260

261

262

DSCOVR NRT data has noticeably fewer data gaps per year than its ACE counterpart, particularly considering the plasma data. However, we do see the same patterns, with sub-five-minute data gaps being the most frequently observed, and the plasma data exhibiting more numerous gaps per year than the magnetic field. For instance, there were around 10,000 sub-five-minute data gaps per year in the plasma data, while there are approximately 4000 per year in the NRT magnetic field data. If we consider the equivalent distributions for both the DSCOVR scientific magnetic field and plasma data, we see fewer gaps of less than five minutes, but additional gaps of an hour or longer, suggesting that - as with ACE - longer periods of data are later discarded.

263

#### 3.2.2 Windowed Data Validity

264

265

266

267

268

269

270

271

272

273

Space weather models often require continuous data as an input, and many numerical or computational techniques will not return a result should even a single entry be missing. For example, a model may require a window of 30 minutes of continuous solar wind data as an input (c.f. A. W. Smith, Forsyth, Rae, Garton, et al., 2021). It is therefore important to examine the fraction of input data windows that gaps would invalidate. This is examined in Figure 4, for the ACE (top) and DSCOVR (bottom) NRT data, plotted in green. In Figure 4 the windows are evaluated as they would present in an operational setting, such that the stride between adjacent windows of data is equal to the cadence of the data (one minute), and therefore the intervals of data tested overlap.

274

275

When using the ACE NRT data (Figure 4a, b), we can see that if five minutes or fewer of continuous data are required (i.e. the model requires an interval of five minutes



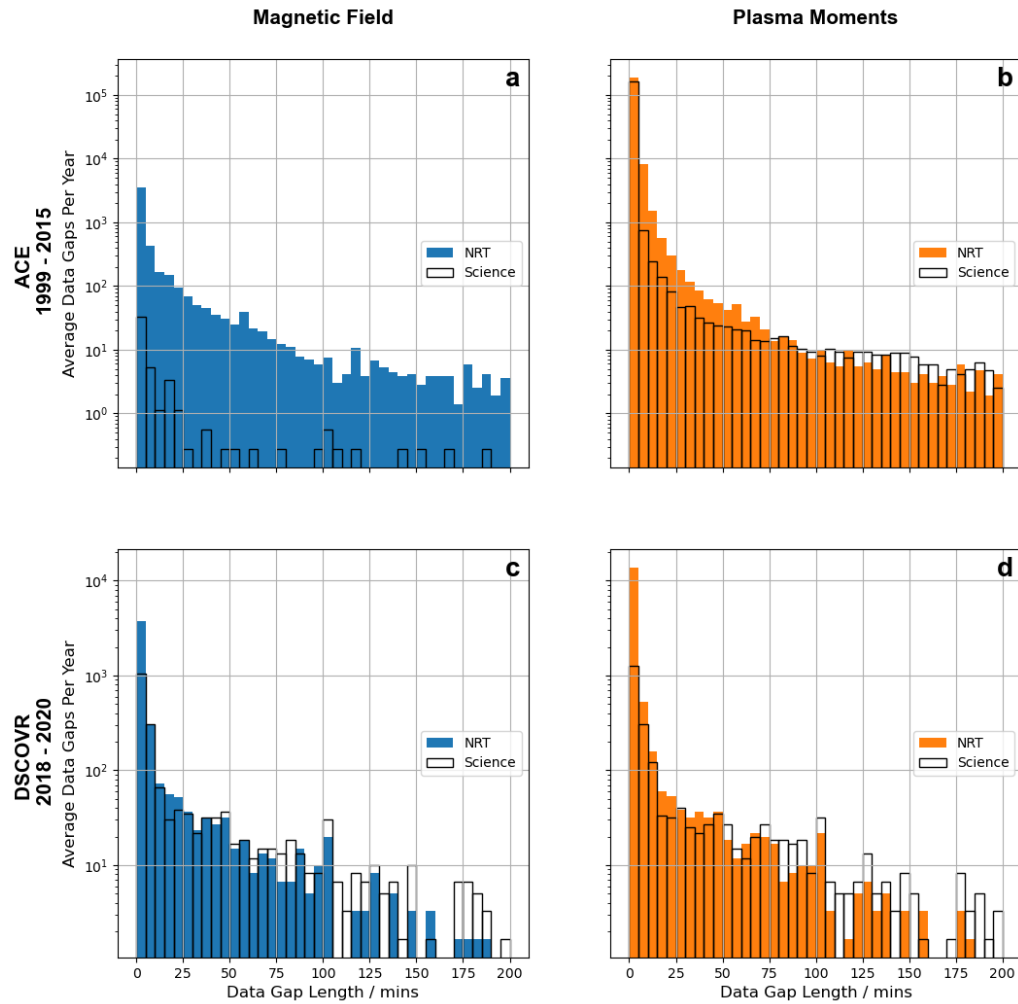


**Figure 3.** The average yearly occurrence of data gaps of different lengths for the ACE (top: a, b) and DSCOVR (bottom: c, d) NRT data, over 16 and 3 years respectively. This is shown for the magnetic field data (left: a, c) and plasma moments (right: b, d). The results for the science data are provided in black. Note the logarithmic y-axes.

of solar wind data as input) then around 90% of the magnetic field data will be available. However, should plasma data also be required then only 55% of input data are valid. As the required length of input window increases, the percentage of valid data intervals decreases. If two hours (120 minutes) of continuous input are required then only 75% of magnetic field data suffice, and approximately 1% of plasma data are available.

Comparatively, DSCOVR NRT data are more complete (Figure 4c, d), noting the different vertical axis scale. For DSCOVR, should a five minute window of data be required then 97% of magnetic field data and 96% of plasma data will be valid. Again, this decreases with longer input window lengths, reaching 86% of magnetic field and 72% of plasma data as the input window length reaches 120 minutes. While this represents a major improvement on ACE, it still has the potential to be a serious issue for forecasting models.

Given how common we have shown short data gaps to be in the NRT data (Figure 3), it is useful to consider how the use of interpolation schemes can increase the quantity of valid, continuous windows of data. Figure 4 shows the application of two maximum lengths of interpolation, in addition to the use of the “raw” data. We can see that if gaps of five minutes or fewer are interpolated (orange stars in Figure 4) then the fraction of valid data intervals increases significantly for both spacecraft and types of data. If the interpolation is permitted over larger gaps of 15 minutes or less (blue crosses in Figure 4) then the fractions increase again, though this is a smaller improvement than was found for the change from the raw data to interpolation over five minutes or less.

#### 4 Example NRT Forecasting of Ground Magnetic Activity

We now qualitatively compare space weather forecast models using science quality data and NRT data. The example model we use is the CNN-based (Convolutional Neural Network) model developed by A. W. Smith, Forsyth, Rae, Garton, et al. (2021), designed to provide a probabilistic forecast as to whether the rate of change of the ground magnetic field ( $R$ ) would exceed certain fixed thresholds at an observatory on the ground (i.e. may be linked to an enhanced GIC risk). In these examples we use the magnetic field at the LER (Lerwick) magnetometer station in Scotland as our target. For full model details the interested reader is directed to A. W. Smith, Forsyth, Rae, Garton, et al. (2021).

The models were trained on data between 2003 and 2014, with 1998 to 2002 being used as a validation set during training. This means that the data from 2015 and 2016 can be used as an unseen test of model performance, e.g. the selected storms discussed below. The models require copious amounts of data to train, covering as complete a record of possible solar wind conditions as can be sourced, and thus we are limited to the ACE datasets. Training a model on the combined ACE and DSCOVR datasets is beyond the scope of this work. Following on from Section 3.2, we interpolate linearly over gaps smaller than 15 minutes in order to maximize the data availability, and perform this consistently for both the ACE NRT and science data. We note that in an NRT data situation we will not necessarily know the next available value as the more recent time intervals may have no data, but we can repeat the last recorded value for a short interval of time. A forecast horizon of 180 minutes has been used for both models.

First, we show the 17th/18th March 2015 St Patrick’s Day storm in Figure 5, which has been previously noted for its ionospheric (e.g. Astafyeva et al., 2015) and ground impacts (e.g. Carter et al., 2016; Kozyreva et al., 2018). We can compare the NRT and science data in the top three panels of Figure 5, from which we can observe some of the results previously discussed in Section 3. It is clear from the velocity and density that there is more rapid temporal variability in the NRT data than is seen in the post-processed ACE data (i.e. Figure 5a, c compared to Figure 5b, d). This short term-variability would explain some of the scatter in Figures 1. There are also significant data gaps in the sci-

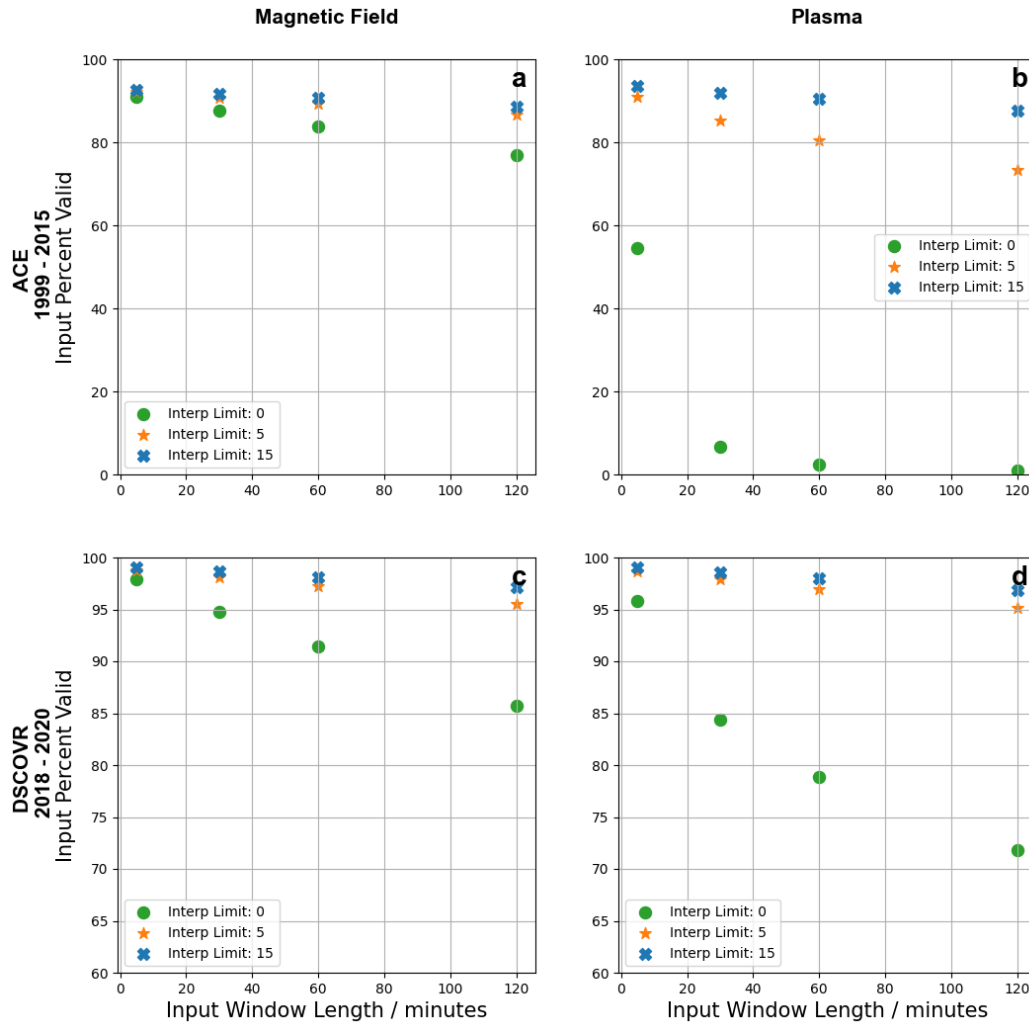


**Figure 4.** The fraction of data windows that are continuous, without data gaps for the ACE (top: a, b) and DSCOVR (bottom: c, d) NRT data. The results for the magnetic field (left: a, c) and plasma data (right: b, d) are shown. The fraction of complete data windows are provided as a function of input window length required to be continuous. Three different interpolation schemes are presented: no interpolation (green circles), interpolation of gaps 5 minutes or shorter (orange stars) and interpolation of gaps 15 minutes or shorter (blue crosses).

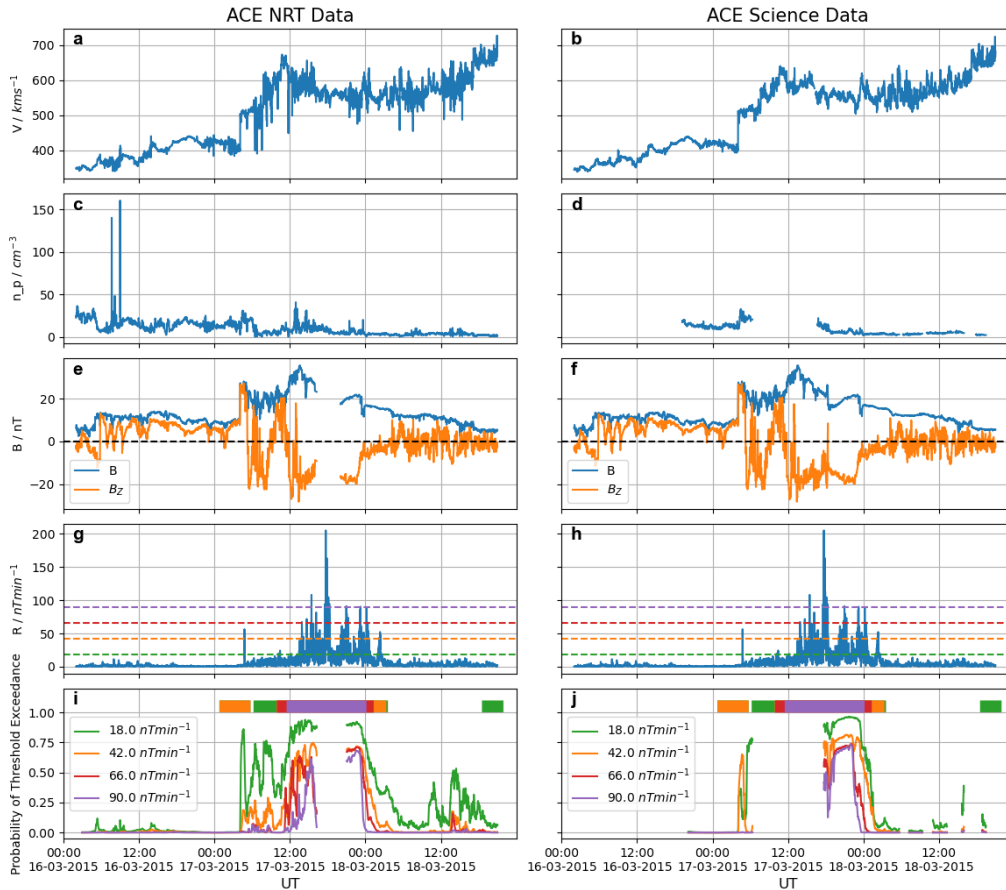


**Figure 5.** Space weather model forecasts produced during a geomagnetic storm in March 2015. ACE NRT data and the relevant model are shown on the left (a, c, e, g, i), while the scientific ACE data and relevant model are on the right (b, d, f, h, j). The solar wind velocity, density, magnetic field strength and  $B_z^{GSM}$  are shown in the top three panels (a, b, c, d, e, f), while the rate of change of the horizontal ground magnetic field observed at LER ( $R$ ) is shown in the fourth panel (g, h). Four model variants are shown, forecasting whether four thresholds of  $R$  will be exceeded (horizontal lines in panels g, h). The bottom panels (i, j) show the model predictions, while the horizontal bars indicate the perfect forecast and the 'maximum' threshold exceeded.

ence density data that are not present in the NRT data (e.g. a few hours around 1200  
 326 UT on the 17th March), suggesting that this data was later removed. On the other hand,  
 327 there is a data gap in the NRT magnetic field data that appears to have been filled with  
 328 further post-processing (e.g. around 1800 UT on the 17th March). Overall, there is an  
 329 extended period during this storm when both the NRT and science-based models are un-  
 330 able to produce a forecast, corresponding to a gap in the NRT magnetic field data and  
 331 the scientific density data, emphasizing the operational challenges in providing space weather  
 332 forecasts. This appears to be precisely the kind of interval when predictions of large ground  
 333 magnetic field variability would be desirable. Nonetheless, both models show increased  
 334 probabilities during the storm, qualitatively reflecting the ground truth.  
 335

336 Next, we show a second example geomagnetic storm (Figure 6), this time on the  
 337 22nd/23rd June 2015, which was notably observed to have adverse impacts on a mid-

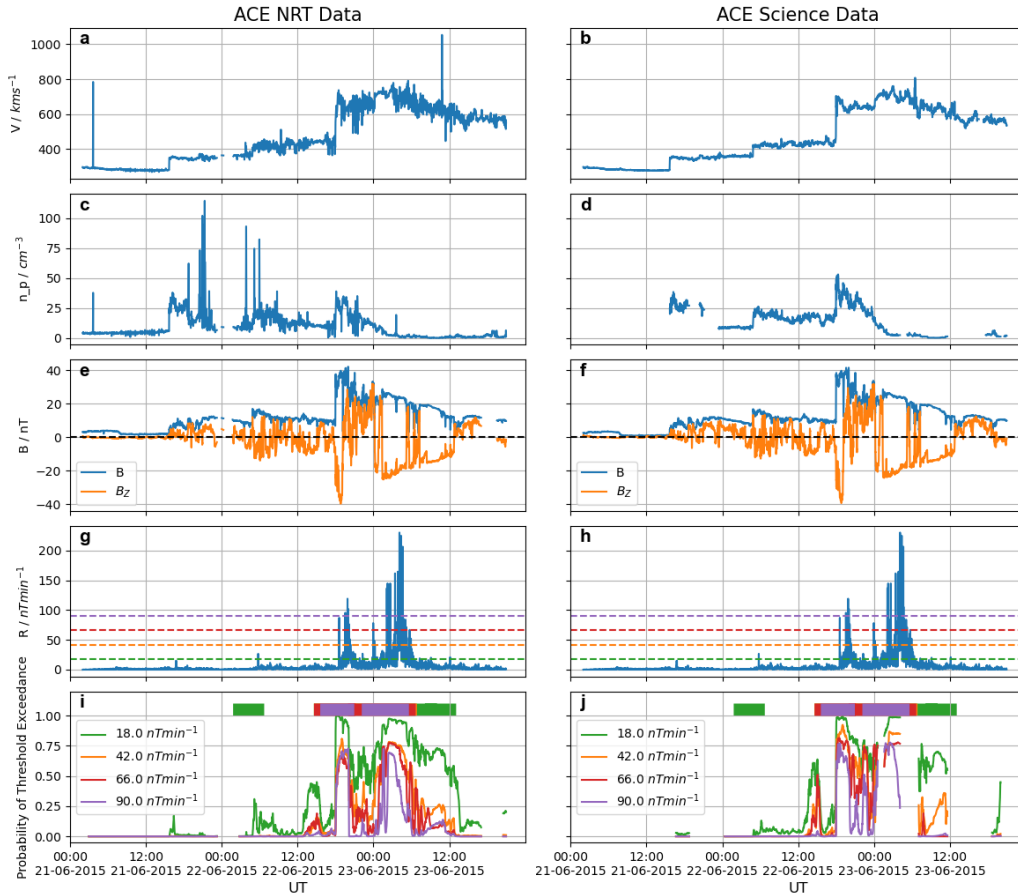


**Figure 6.** Space weather model forecasts produced during a geomagnetic storm in June 2015, with the same format as Figure 5.

latitude railway system (Liu et al., 2016). This storm offers opportunities to further explore several similarities and differences between the scientific and NRT driven models. The increased short-term variability present in the NRT data is once again apparent, and significant intervals of the density data on the 21st June are not present. Inspecting the NRT solar wind velocity data (Figure 6a) we see two anomalous spikes; at 0400 UT on the 21st June and at 1000 UT on the 23rd June. Naively in the NRT data these may initially resemble very large solar wind shocks, to which space weather models may respond. However, we see that the NRT model does not report increased probabilities around these intervals, presumably as the model has seen this anomalous behavior in the training data and only responds to more sustained changes in the solar wind that are corroborated by changes in other solar wind parameters.

Regarding the predicted model probabilities, from single case studies we cannot quantitatively assess the performance of the models, however we can see that during the period of disturbed ground magnetic field activity during the storm that the models are reporting elevated probabilities, as would be desirable, and the NRT and science-based model results qualitatively appear similar. We may compare the metrics returned by the models when applied to the “unseen” NRT and science data between 2015 and 2016. Figure 7 shows three metrics as a function of threshold of the ground magnetic field: the receiver-operator characteristic (ROC), precision-recall (PR) score and Brier skill score (BSS). In terms of ROC score, the scientific and NRT models perform very similarly, while

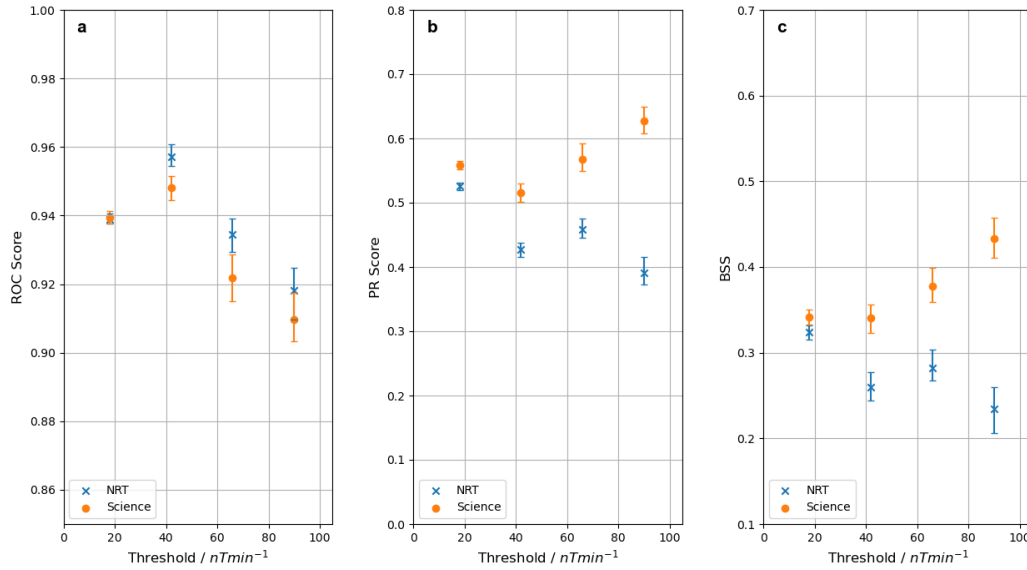


**Figure 7.** Metrics returned by the NRT and Science models when applied to the test data set (2015 - 2016) as a function of threshold of ground magnetic field variability. The receiver-operator characteristic (a), precision-recall (b), and Brier skill score (c) metrics are shown. An input of 60 minutes of solar wind data are used, along with a forecast horizon of 180 minutes (as in Figures 5 and 6). The error bars represent the 95% confidence intervals calculated from 100 iterations of a bootstrap method (with replacement).

in terms of PR and BSS the model based upon the scientific data performs slightly better. We note that due to the presence of different data gaps the metrics are not precisely comparable, and this will be most evident at the highest thresholds which are less frequently exceeded. Nonetheless, the NRT-based model is achieving at least comparable performance to the model employing the science quality data.

## 5 Discussion

The magnetosphere reacts to the impinging solar wind on a range of timescales, and the results are heavily dependent upon the history of the coupled system. For example, even the response to fast changes in solar wind dynamic pressure (e.g. Yue et al., 2010; Shinbori et al., 2012; Oliveira & Raeder, 2015; A. W. Smith, Forsyth, Rae, Rodger, & Freeman, 2021) may be modulated by the magnetospheric state that was induced in the preceding intervals (Zong et al., 2021). Further, characteristic timescales for the response of the currents linking the magnetosphere and ionosphere, and consequent ground magnetic field variability, range from 10s of minutes to several hours (Coxon et al., 2019; Shore et al., 2019). Magnetospheric physics therefore dictates that space weather models need to interpret - in some fashion - the history of the coupled solar wind magnetosphere system. There are two main methods in which models can infer the historical behavior: first, they can use statistical properties of a period of data, such as the variability or range of a solar wind property (e.g. Wintoft et al., 2017; Shprits et al., 2019; Zhelavskaya et al., 2019; Camporeale et al., 2020; A. W. Smith et al., 2020). Second, models can process entire time intervals of data and extract the necessary information themselves (e.g. Kunduri et al., 2020; Keese et al., 2020; A. W. Smith, Forsyth, Rae, Garton, et al., 2021). Discontinuities and unreliable values in the NRT solar wind data thus pose potential risks and limitations to the validity and utility of these models.

**Table 1.** The percentage of magnetic field data with an inconsistent sign in the scientific and NRT data sets.

Magnetic Field Component	ACE	DSCOVR
$B_X^{GSM}$	6.9%	1.8%
$B_Y^{GSM}$	7.4%	1.9%
$B_Z^{GSM}$	12.7%	3.1%

### 5.1 Data Validity

Figures 1 and 2 clearly showed that there are often differences between the reported NRT data and the values that are later found in the post-processed science data. We also showed that the velocity is the most reliable plasma moment returned by the NRT data, compared to the density and temperature. Regarding the magnetic field, while there is considerable spread in the reported magnetic field components, the total magnetic field magnitude is mostly within 10% of the reported NRT value. Meanwhile, we note the limited interval for which DSCOVR data were available has constrained the solar wind conditions to which DSCOVR has been exposed. On inspection, we showed examples of two types of “error” that are present in the NRT data: first, the NRT data tend to exhibit short time scale variability that can be resolved with post-processing; second, there are occasionally very transient anomalous values present in the data (e.g. spikes, Figure 6).

These factors have strong implications for space weather model design and development. The differences between the science and NRT data suggest that - as is best practice - models should be trained upon the data type that will be used in the future. For example, the larger short term variability of the NRT data will need to be found in both the training and evaluation data. We showed that in Figures 5 and 6, the selected model was able to compensate for the additional short-timescale variability in the NRT data. Additionally, artifacts in the data (such as the anomalous spikes in Figure 6) may also be tolerated by some models. However, this is a particular problem if a statistical parameter such as the range of the solar wind velocity is evaluated (e.g. Zhelavskaya et al., 2019; A. W. Smith et al., 2020). This may require simple additional processing of the NRT data, e.g. through smoothing or averaging, prior to its use by a forecasting model.

Space weather models may employ solar wind-magnetosphere coupling functions (e.g. Newell et al., 2007; Milan et al., 2012) in order to assess the geoeffectiveness of the solar wind (e.g. Tan et al., 2018). We note that the selection of coupling function requires careful consideration of the magnetospheric prediction to be made (Lockwood & McWilliams, 2021; Lockwood, 2022). However, one commonality between the various coupling functions is their reliance on the orientation of the interplanetary magnetic field, and therefore the relative sign and value of  $B_Y^{GSM}$  and  $B_Z^{GSM}$ , in particular. As we have shown in Figure 2, particularly with the ACE NRT data, the reliability of these components must be considered with care. Of greatest concern are instances showing evidence of  $B_Y^{GSM}$  and  $B_Z^{GSM}$  changing sign upon further processing/calibration (e.g. data in the upper left or lower right quadrants of Figure 2). Table 1 shows the percentage of magnetic field data that has an inconsistent sign between the scientific and NRT data sets. We can see that the fractions are quite considerable, and that - as in the previous evaluations - the DSCOVR data are more consistent than that from ACE. The reliability (and short term variability) in other NRT solar wind parameters, such as the density, should also be considered. These would result in large fluctuations of the coupling functions that would not be present in the post-processed science data.

## 5.2 Data Continuity

To provide a useful and practical NRT forecast of geomagnetic conditions it is important to maximize the length of time for which it is available. Many magnetospheric models require several hours of historical measurements order to provide a result (e.g. Wintoft et al., 2015; Bortnik et al., 2016; Keesee et al., 2020; A. W. Smith, Forsyth, Rae, Garton, et al., 2021; McGranaghan et al., 2020). The implementation of such models requires careful design, given the nature of the input data available. Additionally, many space weather models will also wish to maximize the data available to allow the largest possible training data sets.

In this work we have shown that data gaps are more numerous in the NRT data sourced from ACE than they are in the data from DSCOVR. Therefore, if only a limited quantity of training data is required then the DSCOVR data would appear to be a good choice. However, the ACE NRT data covers a much longer period of time. This is important as heliospheric conditions and space weather vary over the solar cycle (Luhmann et al., 2002; Chapman et al., 2018, 2020) and between cycles (Lockwood et al., 2014; Hajra et al., 2021; Reyes et al., 2021), while rare, extreme events are the most concerning (Thomson et al., 2011; Kilpua et al., 2015; Vennerstrom et al., 2016; Wintoft et al., 2016; Owens et al., 2021). For this reason, the longer time-span ACE NRT data is an appealing training data set despite its limitations.

We also showed that short data gaps are the most common, for both ACE and DSCOVR NRT data. These frequent but short data gaps significantly impair the continuity of the data. For example, if an hour of continuous data is required as a model input then only 3% of ACE NRT plasma data is valid (Figure 4b). A simple solution is to interpolate over short data gaps. Interpolating over gaps of five minutes or less significantly increases the portion of valid ACE NRT plasma data to 80% (if an hour of continuous data is required). Previous forecasting models, using the somewhat analogous one-minute resolution OMNI data, have applied simple linear interpolations over gaps of 10 (Keesee et al., 2020) or 15 minutes (Wintoft et al., 2015; A. W. Smith, Forsyth, Rae, Garton, et al., 2021) to good effect. Figure 4 also shows that the data gaps are far more prevalent in the plasma data, and so models have been developed that only use the magnetic field data (e.g. Wintoft et al., 2015). Such models may give slightly impaired performance, but they would allow forecasts to be produced during times when the more complete models would otherwise be unavailable. Additionally, techniques such as sub-sampling of the available data (e.g. McGranaghan et al., 2020) may be implemented in such a way as to reduce the effects of short data gaps.

While space weather forecasts have often employed simple (e.g. linear) interpolation methods, reconstructions of the solar wind data using statistical methods have also shown great promise (Kondrashov et al., 2014). A “pattern matching” approach could also be employed to identify historical analogous intervals to provide a surrogate input (c.f. Haines et al., 2021). Meanwhile, longer time-scale reconstruction of solar wind data has also been performed using ground based indices (Machol et al., 2013; Kataoka & Nakano, 2021) and magnetosheath data (Nabert et al., 2015). However, while ground magnetometer data may be available in near-real time, filling NRT data gaps with such reconstructions may be challenging in an operational forecast.

If interpolation is employed then it is useful to consider the solar wind autocorrelation timescales, in order to maximize the data available while minimizing the impact of the interpolation on the quality of the input data. The autocorrelation describes how similar a time series is with a lagged version of itself, and is evaluated for a series of different time offsets, or lags (Appendix A). Figures 8a and 8b show the autocorrelation and partial autocorrelation of four selected NRT solar wind parameters. We will assess these qualitatively. The precise autocorrelations depend on solar wind conditions, but such an analysis is beyond the scope of this work. The autocorrelations have been cal-



474 culated for the longest continuous intervals of DSCOVR NRT data, though we note that  
475 the results do not change significantly based upon the time period selected (so long as  
476 it is of sufficient duration and includes both dynamic and quiescent solar wind).

477 The solar wind properties tested all show significant autocorrelations beyond the  
478 60 minutes shown in Figure 8I, though we do see that the autocorrelation of  $B_Z^{GSM}$  has  
479 nearly reduced to the 95% confidence bound by 60 minutes. This suggests that - in a broad  
480 statistical sense - gaps shorter than 60 minutes could be reasonably interpolated. How-  
481 ever, this completely neglects the importance of short-timescale variability in the cou-  
482 pling of the solar wind and magnetosphere, for example rapid changes in parameters found  
483 during phenomena such as interplanetary shocks. Therefore, while quiescent solar wind  
484 data may undoubtedly be interpolated over relatively large intervals, such large inter-  
485 polation is unadvised during the active intervals of most importance to space weather  
486 models.

487 An additional complication is created if the data gap is present in the most recently  
488 acquired NRT data. Consequently there will be no opportunity to interpolate (e.g. lin-  
489 early) as one side of the data gap is unknown. In this case techniques such as repeat-  
490 ing the last recorded value can be performed, and we should consider the partial auto-  
491 correlation: it ignores the data within the lag period (i.e. it treats the lag period as a  
492 gap). For the solar wind velocity and density (Figure 8a II and b II) the partial auto-  
493 correlations diminish rapidly, and are within the 95% confidence intervals by around 15  
494 and 5 minutes, respectively. Meanwhile, for the solar wind magnetic field magnitude and  
495  $B_Z^{GSM}$  (Figure 8c II and d II) the significant partial autocorrelation timescales are short  
496 at around 8 and 5 minutes, respectively. From this we can conclude that - again a sta-  
497 tistical sense - repeating the last recorded value for approximately five minutes will not  
498 hugely impact the data quality, while performing this for 15 minutes or more will begin  
499 to become problematic, particularly in active geomagnetic conditions.

500 It would be possible to use this kind of analysis to set variable interpolation lim-  
501 its separately for the magnetic field and plasma data, if models only required one type  
502 of data (c.f. Wintoft et al., 2015). We emphasize that these are statistical results on a  
503 long time interval of continuous data, and therefore likely not representative of more ex-  
504 treme or highly transient solar wind conditions under which data gaps may be more likely  
505 (for example due to instrument saturation effects). Additionally, these autocorrelations  
506 have been calculated from the NRT data which, given the short-time scale variability we  
507 have shown above, may cause this to underestimate the “true” solar wind autocorrela-  
508 tion timescales. Nonetheless, these provide a useful estimate of approximate interpola-  
509 tion timescales for the NRT data.

510 Generally, linear interpolations have been employed in the past (e.g. Wintoft et al.,  
511 2015; A. W. Smith, Forsyth, Rae, Garton, et al., 2021), however in the future more com-  
512 plex interpolation methods may give more confidence to interpolating over larger data  
513 gaps, for example using similar historical analogues (Haines et al., 2021), or the use of  
514 auto-regressive models, given the high level of autocorrelation observed. Nonetheless, fu-  
515 ture space weather missions should look to minimize NRT data gaps, those due to in-  
516 strument saturation effects for example (e.g. Nicolaou et al., 2020).

## 517 6 Summary and Conclusions

518 Space weather hazards pose a severe threat to infrastructure such as electricity net-  
519 works. Recognizing this threat, models have been developed to forecast magnetospheric  
520 parameters, such as indices (Tan et al., 2018; Tasistro-Hart et al., 2021; Chakraborty &  
521 Morley, 2020) or direct space weather consequences such as auroral-related particle pre-  
522 cipitation (McGranaghan et al., 2020), radiation belt enhancements (Forsyth et al., 2020),  
523 or ground magnetic perturbations (Wintoft et al., 2015; Keese et al., 2020; A. W. Smith,

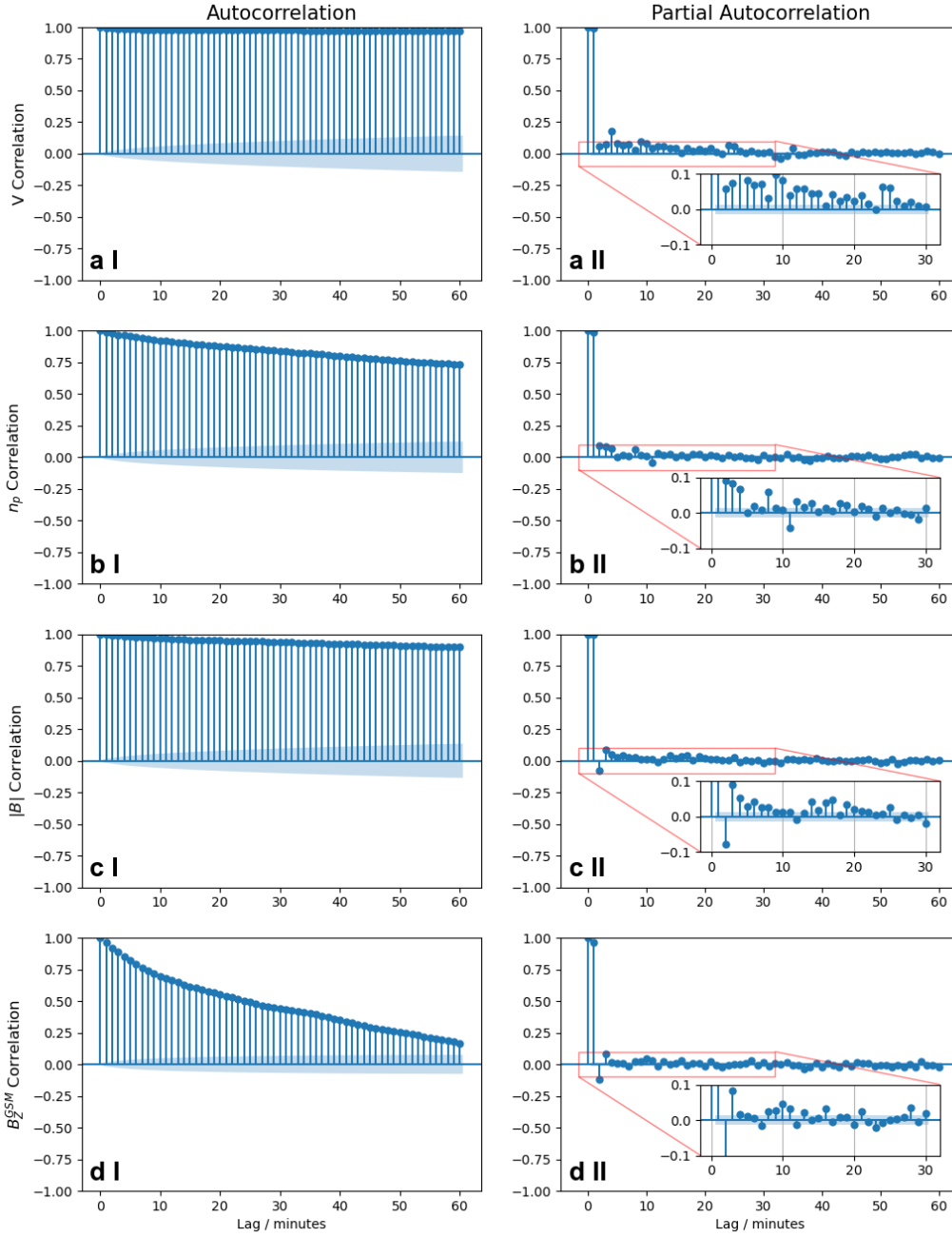


**Figure 8.** The autocorrelation (left, I) and partial autocorrelation (right, II) of four NRT solar wind measurements made by DSCOVR. The autocorrelations for the solar wind velocity ( $V$ , a), proton density ( $n_p$ , b), magnetic field magnitude ( $|B|$ , c) and  $B_z^{GSM}$  component of the magnetic field (d) are presented. The shaded blue regions represent the 95% confidence bound within which points exhibit no significant autocorrelation. The autocorrelations were evaluated during the longest periods of continuous data present between 2018 and 2020 (inclusive). For the plasma properties (a, b) the autocorrelations were calculated on 350 hours of data between 01/05/18 and 16/05/18, while for the magnetic field properties (c, d) the autocorrelations were evaluated for 370 hours of data between 29/05/19 and 13/06/19.

524 Forsyth, Rae, Garton, et al., 2021). Such space weather models are most often trained  
 525 and evaluated on post-processed scientific quality data from spacecraft upstream of the  
 526 Earth at the L1 point. In this work we have assessed the validity and continuity of the  
 527 Near-Real-Time (NRT) data that is available much more rapidly, and showed an exam-  
 528 ple of a forecasting model using such data.

529 When the NRT data are compared to the post-processed, science quality data we  
 530 found that the NRT data are subject to greater short-term variability and occasional anom-  
 531 alous values. Nonetheless, the solar wind velocity is mostly accurate to within  $\pm 10\%$ . While  
 532 the NRT solar wind density and temperature are generally close to the more processed  
 533 values, they are also subject to greater uncertainty. Regarding the magnetic field, the  
 534 total field magnitude is generally reported to within 10% of its processed value. Mean-  
 535 while, there is a greater spread in the individual components of the field, including some  
 536 occasions when the sign of the  $B_Y^{GSM}$  and  $B_Z^{GSM}$  is later corrected. Some models may  
 537 be able to compensate for the differences between the science quality and NRT data (if  
 538 they are trained on the appropriate data source), while others may require additional  
 539 data pre-processing.

540 When considering an operational space weather model it is important to maximize  
 541 its availability. To this end we investigated the occurrence and lengths of data gaps that  
 542 could impede an operational model. We found that short data gaps are frequently found  
 543 in the NRT data, and are more numerous in the plasma data (compared to the magnetic  
 544 field data). Additionally, DSCOVR NRT data shows gaps less frequently than the NRT  
 545 data from ACE. Nonetheless, short interpolations (e.g. over gaps of five minutes or less)  
 546 can dramatically increase data and hence model availability, even when long continuous  
 547 windows are required.

## 548 Appendix A Autocorrelation Analysis

549 In Figure 8 we evaluate the autocorrelation functions of several solar wind param-  
 550 eters. Practically, we employ the python statsmodels package. Theoretically, if we let  
 551  $x_1, x_2, \dots, x_n$  be the observations of a sample of the time series, we take the mean of the  
 552 time series as:

$$\bar{x} = \frac{1}{n} \sum_{t=1}^n x_t \quad (\text{A1})$$

553 The sample auto-covariance function for lag  $h$  ( $h < n$ ) is then defined as:

$$\hat{\gamma}(h) = n^{-1} \sum_{t=1}^{n-h} (x_{t+h} - \bar{x})(x_t - \bar{x}) \quad (\text{A2})$$

554 We then take the sample autocorrelation function for lag  $h$  as:

$$\hat{\rho}(h) = \frac{\hat{\gamma}(h)}{\hat{\gamma}(0)} \quad (\text{A3})$$

555 Meanwhile, the sample partial autocorrelation is the sample autocorrelation between  
 556  $x_t$  and  $x_{t+h}$  but with the linear dependence of  $x_t$  on  $x_{t+1}$  through  $x_{t+h-1}$  removed. For  
 557 more details the interested reader is directed to Brockwell and Davis (2002).

## Acknowledgments

We acknowledge and thank the ACE and DSCOVR teams for the solar wind data and NASA GSFC's Space Physics Data Facility's CDAWeb service for data availability.

Information on the NRT solar wind data may be found at <https://www.swpc.noaa.gov/products/real-time-solar-wind>, while we use data provided by SWPC but archived by the BGS (British Geological Survey) which may be found at the UK NGDC <https://webapps.bgs.ac.uk/services/ngdc/accessions/index.html#item172549>.

Scientific DSCOVR data may be accessed at <https://cdaweb.gsfc.nasa.gov/pub/data/dscovr/>, while the scientific ACE data may be accessed at <https://cdaweb.gsfc.nasa.gov/pub/data/ace/>.

The authors would like to thank Howard Singer for helpful discussions and suggestions.

AWS, CF and IJR were supported by NERC grants NE/P017150/1 and NE/V002724/1. CF was also supported by the NERC Independent Research Fellowship NE/N014480/1. JPE and MJH were supported by NERC grant NE/V003070/1. CMJ was supported by the Science Foundation Ireland (SFI) Grant 18/FRL/6199. AWPT, CDB and GSR are supported by NERC award NE/V002694/1 (SWIMMR Activities in Ground Effects, SAGE).

The analysis in this paper was performed using python, including the TensorFlow (Abadi et al., 2015), pandas (McKinney, 2010), numpy (Van Der Walt et al., 2011), scikit-learn (Pedregosa et al., 2011), scipy (Virtanen et al., 2020) and matplotlib (Hunter, 2007) libraries.

## References

- Abadi, M., Agarwal, A., Barham, P., Brevdo, E., Chen, Z., Citro, C., ... Research, G. (2015). TensorFlow: Large-Scale Machine Learning on Heterogeneous Distributed Systems.. Retrieved from [www.tensorflow.org](http://www.tensorflow.org).
- Aellig, M. R., Lazarus, A. J., Kasper, J. C., & Ogilvie, K. W. (2001). Rapid Measurements of Solar Wind Ions with the Triana PlasMag Faraday Cup. *Astrophysics and Space Science*, 277(1/2), 305–307. Retrieved from <http://link.springer.com/10.1023/A:1012229729242> doi: 10.1023/A:1012229729242
- Astafyeva, E., Zakharenkova, I., & Förster, M. (2015, oct). Ionospheric response to the 2015 St. Patrick's Day storm: A global multi-instrumental overview. *Journal of Geophysical Research: Space Physics*, 120(10), 9023–9037. Retrieved from <http://doi.wiley.com/10.1002/2015JA021629> doi: 10.1002/2015JA021629
- Baker, D., Belian, R., Higbie, P., Klebesadel, R., & Blake, J. (1987, oct). Deep dielectric charging effects due to high-energy electrons in earth's outer magnetosphere. *Journal of Electrostatics*, 20(1), 3–19. Retrieved from <https://www.sciencedirect.com/science/article/abs/pii/0304388687900829?via%3Dihub> doi: 10.1016/0304-3886(87)90082-9
- Baker, D. N., McPherron, R. L., Cayton, T. E., & Klebesadel, R. W. (1990, sep). Linear prediction filter analysis of relativistic electron properties at 6.6  $\mu$ R  $\int_{sub} E_i / \int_{sub} i / i_i$ . *Journal of Geophysical Research*, 95(A9), 15133. Retrieved from <http://doi.wiley.com/10.1029/JA095iA09p15133> doi: 10.1029/JA095iA09p15133
- Baumann, C., & McCloskey, A. E. (2021, aug). Timing of the solar wind propagation delay between L1 and Earth based on machine learning. *Journal of Space Weather and Space Climate*, 11, 41. Retrieved from <https://www.swsc-journal.org/10.1051/swsc/2021026> doi: 10.1051/swsc/2021026
- Beggan, C. D., Beamish, D., Richards, A., Kelly, G. S., & Alan, A. W. (2013, jul). Prediction of extreme geomagnetically induced currents in the UK

- 607 high-voltage network. *Space Weather*, 11(7), 407–419. Retrieved from  
 608 <https://onlinelibrary.wiley.com/doi/10.1002/swe.20065> doi:  
 609 10.1002/swe.20065
- 610 Blake, S. P., Gallagher, P. T., Campaña, J., Hogg, C., Beggan, C. D., Thom-  
 611 son, A. W., ... Bell, D. (2018). A Detailed Model of the Irish High Volt-  
 612 age Power Network for Simulating GICs. *Space Weather*, 16(11), 1770–  
 613 1783. Retrieved from <https://doi.org/10.1029/2018SW001926> doi:  
 614 10.1029/2018SW001926
- 615 Blake, S. P., Gallagher, P. T., McCauley, J., Jones, A. G., Hogg, C., Campaña,  
 616 J., ... Bell, D. (2016, dec). Geomagnetically induced currents in the Irish  
 617 power network during geomagnetic storms. *Space Weather*, 14(12), 1136–  
 618 1154. Retrieved from <http://doi.wiley.com/10.1002/2016SW001534> doi:  
 619 10.1002/2016SW001534
- 620 Blandin, M., Connor, H. K., Öztürk, D. S., Keesee, A. M., Pinto, V., Mahmud,  
 621 M. S., ... Priyadarshi, S. (2022, may). Multi-Variate LSTM Prediction of  
 622 Alaska Magnetometer Chain Utilizing a Coupled Model Approach.  *Fron-*  
 623 *tiers in Astronomy and Space Sciences*, 9, 80. Retrieved from [https://](https://www.frontiersin.org/articles/10.3389/fspas.2022.846291/full)  
 624 [www.frontiersin.org/articles/10.3389/fspas.2022.846291/full](https://www.frontiersin.org/articles/10.3389/fspas.2022.846291/full) doi:  
 625 10.3389/fspas.2022.846291
- 626 Bolduc, L. (2002, nov). GIC observations and studies in the Hydro-Québec power  
 627 system. *Journal of Atmospheric and Solar-Terrestrial Physics*, 64(16), 1793–  
 628 1802. Retrieved from [http://linkinghub.elsevier.com/retrieve/pii/](http://linkinghub.elsevier.com/retrieve/pii/S1364682602001281)  
 629 [S1364682602001281](http://linkinghub.elsevier.com/retrieve/pii/S1364682602001281) doi: 10.1016/S1364-6826(02)00128-1
- 630 Borovsky, J. E. (2020, aug). What magnetospheric and ionospheric researchers  
 631 should know about the solar wind. *Journal of Atmospheric and Solar-*  
 632 *Terrestrial Physics*, 204, 105271. Retrieved from [https://www.sciencedirect](https://www.sciencedirect.com/science/article/abs/pii/S1364682620300882?via%3Dihub)  
 633 [.com/science/article/abs/pii/S1364682620300882?via%3Dihub](https://www.sciencedirect.com/science/article/abs/pii/S1364682620300882?via%3Dihub) doi:  
 634 10.1016/J.JASTP.2020.105271
- 635 Bortnik, J., Li, W., Thorne, R. M., & Angelopoulos, V. (2016, mar). A unified  
 636 approach to inner magnetospheric state prediction. *Journal of Geophysi-*  
 637 *cal Research A: Space Physics*, 121(3), 2423–2430. Retrieved from [http://](http://doi.wiley.com/10.1002/2015JA021733)  
 638 [doi.wiley.com/10.1002/2015JA021733](http://doi.wiley.com/10.1002/2015JA021733) doi: 10.1002/2015JA021733
- 639 Boteler, D. H. (2021, nov). Modeling Geomagnetic Interference on Rail-  
 640 way Signaling Track Circuits. *Space Weather*, 19(1). Retrieved from  
 641 <https://onlinelibrary.wiley.com/doi/10.1029/2020SW002609> doi:  
 642 10.1029/2020SW002609
- 643 Boteler, D. H., Pirjola, R. J., & Nevanlinna, H. (1998, jan). The effects of geo-  
 644 magnetic disturbances on electrical systems at the Earth's surface. *Advances in*  
 645 *Space Research*, 22(1), 17–27. Retrieved from [http://linkinghub.elsevier](http://linkinghub.elsevier.com/retrieve/pii/S027311779701096X)  
 646 [.com/retrieve/pii/S027311779701096X](http://linkinghub.elsevier.com/retrieve/pii/S027311779701096X) doi: 10.1016/S0273-1177(97)01096  
 647 -X
- 648 Brockwell, P. J., & Davis, R. A. (2002). *Introduction to Time Series and Forecasting*  
 649 *- Second Edition*. Retrieved from [http://home.iitj.ac.in/~sim\\$parmod/](http://home.iitj.ac.in/~sim$parmod/document/introductiontimeseries.pdf)  
 650 [document/introductiontimeseries.pdf](http://home.iitj.ac.in/~sim$parmod/document/introductiontimeseries.pdf)[http://books.google.com/](http://books.google.com/books?id=9tv0taI8l6YC)  
 651 [books?id=9tv0taI8l6YC](http://books.google.com/books?id=9tv0taI8l6YC)
- 652 Campbell, W. H. (1980, may). Observation of electric currents in the Alaska oil  
 653 pipeline resulting from auroral electrojet current sources. *Geophysical Journal*  
 654 *International*, 61(2), 437–449. Retrieved from [https://academic.oup.com/](https://academic.oup.com/gji/article-lookup/doi/10.1111/j.1365-246X.1980.tb04325.x)  
 655 [gji/article-lookup/doi/10.1111/j.1365-246X.1980.tb04325.x](https://academic.oup.com/gji/article-lookup/doi/10.1111/j.1365-246X.1980.tb04325.x) doi: 10  
 656 .1111/j.1365-246X.1980.tb04325.x
- 657 Camporeale, E., Cash, M. D., Singer, H. J., Balch, C. C., Huang, Z., & Toth,  
 658 G. (2020, oct). A gray-box model for a probabilistic estimate of regional  
 659 ground magnetic perturbations: Enhancing the NOAA operational Geospace  
 660 model with machine learning. *Journal of Geophysical Research: Space*  
 661 *Physics*. Retrieved from <https://onlinelibrary.wiley.com/doi/10.1029/>

- 2019JA027684 doi: 10.1029/2019JA027684
- 662  
663 Carter, B. A., Yizengaw, E., Pradipta, R., Weygand, J. M., Piersanti, M., Pulkki-  
664 nen, A., ... Zhang, K. (2016, oct). Geomagnetically induced currents  
665 around the world during the 17 March 2015 storm. *Journal of Geophysical*  
666 *Research: Space Physics*, 121(10), 10,496–10,507. Retrieved from [http://](http://doi.wiley.com/10.1002/2016JA023344)  
667 [doi.wiley.com/10.1002/2016JA023344](http://doi.wiley.com/10.1002/2016JA023344) doi: 10.1002/2016JA023344
- 668 Cash, M. D., Witters Hicks, S., Biesecker, D. A., Reinard, A. A., de Koning, C. A.,  
669 & Weimer, D. R. (2016, feb). Validation of an operational product to de-  
670 termine L1 to Earth propagation time delays. *Space Weather*, 14(2), 93–  
671 112. Retrieved from <http://doi.wiley.com/10.1002/2015SW001321> doi:  
672 10.1002/2015SW001321
- 673 Chakraborty, S., & Morley, S. K. (2020, jul). Probabilistic prediction of geomag-  
674 netic storms and the  $\int_{i_0}^{\infty} K_{\text{p}} \int_{\text{sub}} \int_{i_0}^{\infty} / i_0$  index. *Journal of Space Weather*  
675 *and Space Climate*, 10, 36. Retrieved from [https://www.swsc-journal.org/](https://www.swsc-journal.org/10.1051/swsc/2020037)  
676 [10.1051/swsc/2020037](https://www.swsc-journal.org/10.1051/swsc/2020037) doi: 10.1051/swsc/2020037
- 677 Chapman, S. C., McIntosh, S. W., Leamon, R. J., & Watkins, N. W. (2020,  
678 jun). Quantifying the Solar Cycle Modulation of Extreme Space Weather.  
679 *Geophysical Research Letters*, 47(11), e2020GL087795. Retrieved from  
680 <https://onlinelibrary.wiley.com/doi/10.1029/2020GL087795> doi:  
681 10.1029/2020GL087795
- 682 Chapman, S. C., Watkins, N. W., & Tindale, E. (2018, aug). Reproducible As-  
683 pects of the Climate of Space Weather Over the Last Five Solar Cycles. *Space*  
684 *Weather*, 16(8), 1128–1142. Retrieved from [http://doi.wiley.com/10.1029/](http://doi.wiley.com/10.1029/2018SW001884)  
685 [2018SW001884](http://doi.wiley.com/10.1029/2018SW001884) doi: 10.1029/2018SW001884
- 686 Chu, X., Ma, D., Bortnik, J., Tobiska, W. K., Cruz, A., Bouwer, S. D., ... Reeves,  
687 G. (2021, dec). Relativistic Electron Model in the Outer Radiation Belt Us-  
688 ing a Neural Network Approach. *Space Weather*, 19(12), e2021SW002808.  
689 Retrieved from [https://onlinelibrary.wiley.com/doi/10.1029/](https://onlinelibrary.wiley.com/doi/10.1029/2021SW002808)  
690 [2021SW002808](https://onlinelibrary.wiley.com/doi/10.1029/2021SW002808) doi: 10.1029/2021SW002808
- 691 Coxon, J. C., Shore, R. M., Freeman, M. P., Fear, R. C., Browett, S. D., Smith,  
692 A. W., ... Anderson, B. J. (2019, jul). Timescales of Birkeland Cur-  
693 rents Driven by the IMF. *Geophysical Research Letters*, 46(14), 7893–  
694 7901. Retrieved from [https://onlinelibrary.wiley.com/doi/10.1029/](https://onlinelibrary.wiley.com/doi/10.1029/2018GL081658)  
695 [2018GL081658](https://onlinelibrary.wiley.com/doi/10.1029/2018GL081658) doi: 10.1029/2018GL081658
- 696 Dimmock, A. P., Rosenqvist, L., Hall, J. O., Viljanen, A., Yordanova, E., Honkonen,  
697 I., ... Sjöberg, E. C. (2019, jun). The GIC and Geomagnetic Response Over  
698 Fennoscandia to the 7–8 September 2017 Geomagnetic Storm. *Space Weather*,  
699 17(7), 989–1010. Retrieved from [https://onlinelibrary.wiley.com/doi/](https://onlinelibrary.wiley.com/doi/abs/10.1029/2018SW002132)  
700 [abs/10.1029/2018SW002132](https://onlinelibrary.wiley.com/doi/abs/10.1029/2018SW002132) doi: 10.1029/2018SW002132
- 701 Dimmock, A. P., Welling, D. T., Rosenqvist, L., Forsyth, C., Freeman, M. P.,  
702 Rae, I. J., ... Yordanova, E. (2021, apr). Modeling the Geomagnetic Re-  
703 sponse to the September 2017 Space Weather Event Over Fennoscandia Us-  
704 ing the Space Weather Modeling Framework: Studying the Impacts of Spa-  
705 tial Resolution. *Space Weather*, 19(5), e2020SW002683. Retrieved from  
706 <https://onlinelibrary.wiley.com/doi/10.1029/2020SW002683> doi:  
707 10.1029/2020SW002683
- 708 Divett, T., Mac Manus, D. H., Richardson, G. S., Beggan, C. D., Rodger, C. J., Ing-  
709 ham, M., ... Obana, Y. (2020, jun). Geomagnetically Induced Current Model  
710 Validation From New Zealand’s South Island. *Space Weather*, 18(8). Retrieved  
711 from <https://onlinelibrary.wiley.com/doi/abs/10.1029/2020SW002494>  
712 doi: 10.1029/2020SW002494
- 713 Divett, T., Richardson, G. S., Beggan, C. D., Rodger, C. J., Boteler, D. H., Ingham,  
714 M., ... Dalzell, M. (2018, jun). Transformer-Level Modeling of Geomagneti-  
715 cally Induced Currents in New Zealand’s South Island. *Space Weather*, 16(6),  
716 718–735. Retrieved from <http://doi.wiley.com/10.1029/2018SW001814>

- 717 doi: 10.1029/2018SW001814
- 718 Eastwood, J. P., Hapgood, M. A., Biffis, E., Benedetti, D., Bisi, M. M., Green, L.,  
719 ... Burnett, C. (2018, dec). Quantifying the Economic Value of Space Weather  
720 Forecasting for Power Grids: An Exploratory Study. *Space Weather*, 16(12),  
721 2052–2067. Retrieved from <http://doi.wiley.com/10.1029/2018SW002003>  
722 doi: 10.1029/2018SW002003
- 723 Forsyth, C., Watt, C. E., Mooney, M. K., Rae, I. J., Walton, S. D., & Horne, R. B.  
724 (2020, jun). Forecasting GOES 15  $\geq 2$  MeV Electron Fluxes From Solar Wind  
725 Data and Geomagnetic Indices. *Space Weather*, 18(8). Retrieved from  
726 <https://onlinelibrary.wiley.com/doi/abs/10.1029/2019SW002416> doi:  
727 10.1029/2019SW002416
- 728 Freeman, M. P., Forsyth, C., & Rae, I. J. (2019, may). The influence of  
729 substorms on extreme rates of change of the surface horizontal mag-  
730 netic field in the U.K. *Space Weather*, 2018SW002148. Retrieved from  
731 <https://onlinelibrary.wiley.com/doi/abs/10.1029/2018SW002148> doi:  
732 10.1029/2018SW002148
- 733 Gaunt, C. T., & Coetzee, G. (2007). Transformer failures in regions incorrectly con-  
734 sidered to have low GIC-risk. In *2007 IEEE Lausanne PowerTech, Proceedings* (pp.  
735 807–812). doi: 10.1109/PCT.2007.4538419
- 736 Gleisner, H., & Lundstedt, H. (2001, may). A neural network-based local model  
737 for prediction of geomagnetic disturbances. *Journal of Geophysical Research:  
738 Space Physics*, 106(A5), 8425–8433. Retrieved from [http://doi.wiley.com/  
739 10.1029/2000JA900142](http://doi.wiley.com/10.1029/2000JA900142) doi: 10.1029/2000JA900142
- 740 Grawe, M. A., & Makela, J. J. (2021, jul). Predictability of Geomagnet-  
741 ically Induced Currents as a Function of Available Magnetic Field In-  
742 formation. *Space Weather*, 19(8), e2021SW002747. Retrieved from  
743 <https://onlinelibrary.wiley.com/doi/10.1029/2021SW002747> doi:  
744 10.1029/2021SW002747
- 745 Gummow, R., & Eng, P. (2002, nov). GIC effects on pipeline corrosion and corro-  
746 sion control systems. *Journal of Atmospheric and Solar-Terrestrial Physics*,  
747 64(16), 1755–1764. Retrieved from [https://www.sciencedirect.com/  
748 science/article/pii/S1364682602001256?via%3Dihub](https://www.sciencedirect.com/science/article/pii/S1364682602001256?via%3Dihub) doi: 10.1016/  
749 S1364-6826(02)00125-6
- 750 Haines, C., Owens, M. J., Barnard, L., Lockwood, M., Ruffenach, A., Boykin, K.,  
751 & McGranaghan, R. (2021, may). Forecasting Occurrence and Intensity of  
752 Geomagnetic Activity With Pattern-Matching Approaches. *Space Weather*,  
753 19(6), e2020SW002624. Retrieved from [https://onlinelibrary.wiley.com/  
754 doi/10.1029/2020SW002624](https://onlinelibrary.wiley.com/doi/10.1029/2020SW002624) doi: 10.1029/2020SW002624
- 755 Hajra, R., Franco, A., Echer, E., & Bolzan, M. (2021, apr). Long-Term Varia-  
756 tions of the Geomagnetic Activity: A Comparison Between the Strong and  
757 Weak Solar Activity Cycles and Implications for the Space Climate. *Journal  
758 of Geophysical Research: Space Physics*, 126(4), e2020JA028695. Retrieved  
759 from <https://onlinelibrary.wiley.com/doi/10.1029/2020JA028695> doi:  
760 10.1029/2020JA028695
- 761 Heyns, M. J., Lotz, S. I., & Gaunt, C. T. (2021, nov). Geomagnetic Pulsations  
762 Driving Geomagnetically Induced Currents. *Space Weather*, 19(2). Retrieved  
763 from <https://onlinelibrary.wiley.com/doi/10.1029/2020SW002557> doi:  
764 10.1029/2020SW002557
- 765 Hunter, J. D. (2007). Matplotlib: A 2D graphics environment. *Computing in Science  
766 and Engineering*, 9(3), 90–95. Retrieved from [http://ieeexplore.ieee.org/  
767 document/4160265/](http://ieeexplore.ieee.org/document/4160265/) doi: 10.1109/MCSE.2007.55
- 768 Lucci, N., Levitin, A. E., Belov, A. V., Eroshenko, E. A., Ptitsyna, N. G., Vil-  
769 loresi, G., ... Yanke, V. G. (2005, jan). Space weather conditions and  
770 spacecraft anomalies in different orbits. *Space Weather*, 3(1), n/a–n/a.  
771 Retrieved from <http://doi.wiley.com/10.1029/2003SW000056> doi:

- 772 10.1029/2003SW000056  
 773 Kappenman, J. G., & Albertson, D. (1990, mar). Bracing for the geomag-  
 774 netic storms. *IEEE Spectrum*, 27(3), 27–33. Retrieved from [http://](http://ieeexplore.ieee.org/document/48847/)  
 775 [ieeexplore.ieee.org/document/48847/](http://ieeexplore.ieee.org/document/48847/) doi: 10.1109/6.48847  
 776 Kataoka, R., & Nakano, S. (2021, nov). Reconstructing solar wind profiles associ-  
 777 ated with extreme magnetic storms: A machine learning approach. *Geophysi-*  
 778 *cal Research Letters*, e2021GL096275. Retrieved from [https://onlinelibrary](https://onlinelibrary.wiley.com/doi/10.1029/2021GL096275)  
 779 [.wiley.com/doi/10.1029/2021GL096275](https://onlinelibrary.wiley.com/doi/10.1029/2021GL096275) doi: 10.1029/2021GL096275  
 780 Keesee, A. M., Pinto, V., Coughlan, M., Lennox, C., Mahmud, M. S., & Con-  
 781 nor, H. K. (2020, oct). Comparison of Deep Learning Techniques to  
 782 Model Connections Between Solar Wind and Ground Magnetic Perturba-  
 783 tions. *Frontiers in Astronomy and Space Sciences*, 7, 72. Retrieved from  
 784 <https://www.frontiersin.org/article/10.3389/fspas.2020.550874/full>  
 785 doi: 10.3389/fspas.2020.550874  
 786 Kilpua, E. K., Olsper, N., Grigorievskiy, A., Käpylä, M. J., Tanskanen, E. I., Miya-  
 787 hara, H., ... Liu, Y. D. (2015, jun). Statistical Study of Strong and Extreme  
 788 Geomagnetic Disturbances and Solar Cycle Characteristics. *Astrophysic-*  
 789 *cal Journal*, 806(2), 272. Retrieved from [https://iopscience.iop.org/](https://iopscience.iop.org/article/10.1088/0004-637X/806/2/272)  
 790 [article/10.1088/0004-637X/806/2/272](https://iopscience.iop.org/article/10.1088/0004-637X/806/2/272) doi: 10.1088/0004-637X/806/2/  
 791 272  
 792 Kondrashov, D., Denton, R., Shprits, Y. Y., & Singer, H. J. (2014, apr). Reconstruc-  
 793 tion of gaps in the past history of solar wind parameters. *Geophysical Research*  
 794 *Letters*, 41(8), 2702–2707. Retrieved from [http://doi.wiley.com/10.1002/](http://doi.wiley.com/10.1002/2014GL059741)  
 795 [2014GL059741](http://doi.wiley.com/10.1002/2014GL059741) doi: 10.1002/2014GL059741  
 796 Kozyreva, O. V., Pilipenko, V. A., Belakhovsky, V. B., & Sakharov, Y. A. (2018,  
 797 dec). Ground geomagnetic field and GIC response to March 17, 2015, storm.  
 798 *Earth, Planets and Space*, 70(1), 157. Retrieved from [https://earth-planet-](https://earth-planet-space.springeropen.com/articles/10.1186/s40623-018-0933-2)  
 799 [space.springeropen.com/articles/10.1186/s40623-018-0933-2](https://earth-planet-space.springeropen.com/articles/10.1186/s40623-018-0933-2) doi:  
 800 10.1186/s40623-018-0933-2  
 801 Kunduri, B. S., Maimaiti, M., Baker, J. B., Ruohoniemi, J. M., Anderson, B. J.,  
 802 & Vines, S. K. (2020, aug). A Deep Learning-Based Approach for Mod-  
 803 eling the Dynamics of AMPERE Birkeland Currents. *Journal of Geophys-*  
 804 *ical Research: Space Physics*, 125(8), e2020JA027908. Retrieved from  
 805 <https://onlinelibrary.wiley.com/doi/10.1029/2020JA027908> doi:  
 806 10.1029/2020JA027908  
 807 Liu, L., Ge, X., Zong, W., Zhou, Y., & Liu, M. (2016, oct). Analysis of the moni-  
 808 toring data of geomagnetic storm interference in the electrification system of a  
 809 high-speed railway. *Space Weather*, 14(10), 754–763. Retrieved from [http://](http://doi.wiley.com/10.1002/2016SW001411)  
 810 [doi.wiley.com/10.1002/2016SW001411](http://doi.wiley.com/10.1002/2016SW001411) doi: 10.1002/2016SW001411  
 811 Lockwood, M. (2022, feb). Solar Wind—Magnetosphere Coupling Functions: Pit-  
 812 falls, Limitations, and Applications. *Space Weather*, 20(2), e2021SW002989.  
 813 Retrieved from [https://onlinelibrary.wiley.com/doi/10.1029/](https://onlinelibrary.wiley.com/doi/10.1029/2021SW002989)  
 814 [2021SW002989](https://onlinelibrary.wiley.com/doi/10.1029/2021SW002989) doi: 10.1029/2021SW002989  
 815 Lockwood, M., Bentley, S. N., Owens, M. J., Barnard, L. A., Scott, C. J., Watt,  
 816 C. E., & Allanson, O. (2019, jan). The Development of a Space Climatol-  
 817 ogy: 1. Solar Wind Magnetosphere Coupling as a Function of Timescale and  
 818 the Effect of Data Gaps. *Space Weather*, 17(1), 133–156. Retrieved from  
 819 <https://onlinelibrary.wiley.com/doi/abs/10.1029/2018SW001856> doi:  
 820 10.1029/2018SW001856  
 821 Lockwood, M., & McWilliams, K. A. (2021, nov). On optimum solar wind  
 822 – magnetosphere coupling functions for transpolar voltage and planetary  
 823 geomagnetic activity. *Journal of Geophysical Research: Space Physics*,  
 824 e2021JA029946. Retrieved from [https://onlinelibrary.wiley.com/doi/](https://onlinelibrary.wiley.com/doi/10.1029/2021JA029946)  
 825 [10.1029/2021JA029946](https://onlinelibrary.wiley.com/doi/10.1029/2021JA029946) doi: 10.1029/2021JA029946  
 826 Lockwood, M., Nevanlinna, H., Vokhmyanin, M., Ponyavin, D., Sokolov, S.,



- 827 Barnard, L., . . . Scott, C. J. (2014). Reconstruction of geomagnetic ac-  
 828 tivity and near-Earth interplanetary conditions over the past 167 yrs; Part  
 829 3: Improved representation of solar cycle 11. *Annales Geophysicae*, *32*(4),  
 830 367–381. Retrieved from [www.ann-geophys.net/32/367/2014/](http://www.ann-geophys.net/32/367/2014/) doi:  
 831 10.5194/angeo-32-367-2014
- 832 Love, J. J., Hayakawa, H., & Cliver, E. W. (2019, aug). Intensity and Impact of  
 833 the New York Railroad Superstorm of May 1921. *Space Weather*, *17*(8), 1281–  
 834 1292. Retrieved from [https://onlinelibrary.wiley.com/doi/abs/10.1029/](https://onlinelibrary.wiley.com/doi/abs/10.1029/2019SW002250)  
 835 [2019SW002250](https://onlinelibrary.wiley.com/doi/abs/10.1029/2019SW002250) doi: 10.1029/2019SW002250
- 836 Luhmann, J. G., Li, Y., Arge, C. N., Gazis, P. R., & Ulrich, R. (2002, aug).  
 837 Solar cycle changes in coronal holes and space weather cycles. *Journal*  
 838 *of Geophysical Research: Space Physics*, *107*(A8), SMP 3–1–SMP 3–12.  
 839 Retrieved from <http://doi.wiley.com/10.1029/2001JA007550> doi:  
 840 10.1029/2001JA007550
- 841 Mac Manus, D. H., Rodger, C. J., Dalzell, M., Thomson, A. W. P., Clilverd,  
 842 M. A., Petersen, T., . . . Divett, T. (2017, aug). Long-term geomagnet-  
 843 ically induced current observations in New Zealand: Earth return correc-  
 844 tions and geomagnetic field driver. *Space Weather*, *15*(8), 1020–1038.  
 845 Retrieved from <http://doi.wiley.com/10.1002/2017SW001635> doi:  
 846 10.1002/2017SW001635
- 847 Mac Manus, D. H., Rodger, C. J., Ingham, M., Clilverd, M. A., Dalzell, M., Di-  
 848 vett, T., . . . Petersen, T. (2022). Geomagnetically Induced Current Model in  
 849 New Zealand Across Multiple Disturbances: Validation and Extension to Non-  
 850 Monitored Transformers. *Space Weather*, *20*(2). doi: 10.1029/2021SW002955
- 851 Machol, J. L., Reinard, A. A., Viereck, R. A., & Biesecker, D. A. (2013, jul).  
 852 Identification and replacement of proton-contaminated real-time ACE so-  
 853 lar wind measurements. *Space Weather*, *11*(7), 434–440. Retrieved from  
 854 <http://doi.wiley.com/10.1002/swe.20070> doi: 10.1002/swe.20070
- 855 Marshall, R. A., Dalzell, M., Waters, C. L., Goldthorpe, P., & Smith, E. A. (2012,  
 856 aug). Geomagnetically induced currents in the New Zealand power network.  
 857 *Space Weather*, *10*(8), n/a–n/a. Retrieved from [http://doi.wiley.com/10](http://doi.wiley.com/10.1029/2012SW000806)  
 858 [.1029/2012SW000806](http://doi.wiley.com/10.1029/2012SW000806) doi: 10.1029/2012SW000806
- 859 McComas, D., Bame, S., Barker, P., Feldman, W., Phillips, J., Riley, P., & Griffee,  
 860 J. (1998). Solar Wind Electron Proton Alpha Monitor (SWEPAM) for the  
 861 Advanced Composition Explorer. *Space Science Reviews*, *86*(1/4), 563–612.  
 862 Retrieved from <http://link.springer.com/10.1023/A:1005040232597> doi:  
 863 10.1023/A:1005040232597
- 864 McGranaghan, R. M., Ziegler, J., Bloch, T., Hatch, S., Camporeale, E., Lynch,  
 865 K., . . . Skone, S. (2020, apr). Next generation particle precipitation:  
 866 Mesoscale prediction through machine learning (a case study and frame-  
 867 work for progress). *Space Weather*, e2020SW002684. Retrieved from  
 868 <https://onlinelibrary.wiley.com/doi/10.1029/2020SW002684> doi:  
 869 10.1029/2020SW002684
- 870 McKinney, W. (2010). *Data Structures for Statistical Computing in Python*. Re-  
 871 trieved from [http://conference.scipy.org/proceedings/scipy2010/](http://conference.scipy.org/proceedings/scipy2010/mckinney.html)  
 872 [mckinney.html](http://conference.scipy.org/proceedings/scipy2010/mckinney.html)
- 873 Milan, S. E., Gosling, J. S., & Hubert, B. (2012). Relationship between interplan-  
 874 etary parameters and the magnetopause reconnection rate quantified from  
 875 observations of the expanding polar cap. *Journal of Geophysical Research:*  
 876 *Space Physics*, *117*(3). Retrieved from [https://agupubs.onlinelibrary](https://agupubs.onlinelibrary.wiley.com/doi/pdf/10.1029/2011JA017082)  
 877 [.wiley.com/doi/pdf/10.1029/2011JA017082](https://agupubs.onlinelibrary.wiley.com/doi/pdf/10.1029/2011JA017082) doi: 10.1029/2011JA017082
- 878 Nabert, C., Othmer, C., & Glassmeier, K.-H. (2015, dec). Solar wind reconstruction  
 879 from magnetosheath data using an adjoint approach. *Annales Geophysi-*  
 880 *caae*, *33*(12), 1513–1524. Retrieved from [https://angeo.copernicus.org/](https://angeo.copernicus.org/articles/33/1513/2015/)  
 881 [articles/33/1513/2015/](https://angeo.copernicus.org/articles/33/1513/2015/) doi: 10.5194/angeo-33-1513-2015

- 882 Newell, P. T., Sotirelis, T., Liou, K., Meng, C.-I., & Rich, F. J. (2007, jan). A nearly  
 883 universal solar wind-magnetosphere coupling function inferred from 10 mag-  
 884 netospheric state variables. *Journal of Geophysical Research: Space Physics*,  
 885 *112*(A1). Retrieved from <http://doi.wiley.com/10.1029/2006JA012015>  
 886 doi: 10.1029/2006JA012015
- 887 Nicolaou, G., Wicks, R. T., Rae, I. J., & Kataria, D. O. (2020, dec). Evaluating  
 888 the Performance of a Plasma Analyzer for a Space Weather Monitor Mis-  
 889 sion Concept. *Space Weather*, *18*(12), e2020SW002559. Retrieved from  
 890 <https://onlinelibrary.wiley.com/doi/10.1029/2020SW002559> doi:  
 891 10.1029/2020SW002559
- 892 Oliveira, D. M., & Raeder, J. (2015, jun). Impact angle control of interplanetary  
 893 shock geoeffectiveness: A statistical study. *Journal of Geophysical Research:*  
 894 *Space Physics*, *120*(6), 4313–4323. Retrieved from [http://doi.wiley.com/10](http://doi.wiley.com/10.1002/2015JA021147)  
 895 [.1002/2015JA021147](http://doi.wiley.com/10.1002/2015JA021147) doi: 10.1002/2015JA021147
- 896 Oughton, E. J., Hapgood, M., Richardson, G. S., Beggan, C. D., Thomson, A. W.,  
 897 Gibbs, M., ... Horne, R. B. (2019, may). A Risk Assessment Framework for  
 898 the Socioeconomic Impacts of Electricity Transmission Infrastructure Failure  
 899 Due to Space Weather: An Application to the United Kingdom. *Risk Analysis*,  
 900 *39*(5), 1022–1043. Retrieved from [https://onlinelibrary.wiley.com/doi/](https://onlinelibrary.wiley.com/doi/abs/10.1111/risa.13229)  
 901 [abs/10.1111/risa.13229](https://onlinelibrary.wiley.com/doi/abs/10.1111/risa.13229) doi: 10.1111/risa.13229
- 902 Oughton, E. J., Skelton, A., Horne, R. B., Thomson, A. W. P., & Gaunt, C. T.  
 903 (2017, jan). Quantifying the daily economic impact of extreme space weather  
 904 due to failure in electricity transmission infrastructure. *Space Weather*, *15*(1),  
 905 65–83. Retrieved from <http://doi.wiley.com/10.1002/2016SW001491> doi:  
 906 10.1002/2016SW001491
- 907 Owens, M. J., Lockwood, M., Barnard, L. A., Scott, C. J., Haines, C., & Macneil,  
 908 A. (2021, may). Extreme Space-Weather Events and the Solar Cycle. *Solar*  
 909 *Physics*, *296*(5), 82. Retrieved from [https://link.springer.com/10.1007/](https://link.springer.com/10.1007/s11207-021-01831-3)  
 910 [s11207-021-01831-3](https://link.springer.com/10.1007/s11207-021-01831-3) doi: 10.1007/s11207-021-01831-3
- 911 Pedregosa, F., Varoquaux, G., Gramfort, A., Michel, V., Thirion, B., Grisel, O., ...  
 912 Duchesnay, É. (2011). Scikit-learn: Machine Learning in Python. *Jour-*  
 913 *nal of Machine Learning Research*, *12*(Oct), 2825–2830. Retrieved from  
 914 <http://jmlr.org/papers/v12/pedregosa11a.html>
- 915 Pinto, V. A., Keesee, A. M., Coughlan, M., Mukundan, R., Johnson, J. W., Ng-  
 916 wira, C. M., & Connor, H. K. (2022, may). Revisiting the Ground Mag-  
 917 netic Field Perturbations Challenge: A Machine Learning Perspective.  *Fron-*  
 918 *tiers in Astronomy and Space Sciences*, *9*, 123. Retrieved from [https://](https://www.frontiersin.org/articles/10.3389/fspas.2022.869740/full)  
 919 [www.frontiersin.org/articles/10.3389/fspas.2022.869740/full](https://www.frontiersin.org/articles/10.3389/fspas.2022.869740/full) doi:  
 920 10.3389/fspas.2022.869740
- 921 Pulkkinen, A., Kuznetsova, M., Ridley, A., Raeder, J., Vapirev, A., Weimer, D.,  
 922 ... Chulaki, A. (2011, feb). Geospace Environment Modeling 2008-2009  
 923 Challenge: Ground magnetic field perturbations. *Space Weather*, *9*(2), n/a–  
 924 n/a. Retrieved from <http://doi.wiley.com/10.1029/2010SW000600> doi:  
 925 10.1029/2010SW000600
- 926 Pulkkinen, A., Lindahl, S., Viljanen, A., & Pirjola, R. (2005, aug). Geomagnetic  
 927 storm of 29-31 October 2003: Geomagnetically induced currents and their rela-  
 928 tion to problems in the Swedish high-voltage power transmission system. *Space*  
 929 *Weather*, *3*(8), n/a–n/a. Retrieved from [http://doi.wiley.com/10.1029/](http://doi.wiley.com/10.1029/2004SW000123)  
 930 [2004SW000123](http://doi.wiley.com/10.1029/2004SW000123) doi: 10.1029/2004SW000123
- 931 Pulkkinen, A., Rastätter, L., Kuznetsova, M., Singer, H., Balch, C., Weimer,  
 932 D., ... Weigel, R. (2013, jun). Community-wide validation of geospace  
 933 model ground magnetic field perturbation predictions to support model  
 934 transition to operations. *Space Weather*, *11*(6), 369–385. Retrieved from  
 935 <http://doi.wiley.com/10.1002/swe.20056> doi: 10.1002/swe.20056
- 936 Rajput, V. N., Boteler, D. H., Rana, N., Saiyed, M., Anjana, S., & Shah, M.

- 937 (2020, nov). Insight into impact of geomagnetically induced currents on  
 938 power systems: Overview, challenges and mitigation. *Electric Power Sys-*  
 939 *tems Research*, 106927. Retrieved from [https://www.sciencedirect.com/science/article/pii/S0378779620307252?casa\\_token=Qs4jRHozhEkAAAAA:4AV7PlSDLxVc7NkeV0hvhPk0qJFgVgo0NrejBL7VLzYer8fpctmlt2uGLtyVZsclpbeG\\_U-imEi6](https://www.sciencedirect.com/science/article/pii/S0378779620307252?casa_token=Qs4jRHozhEkAAAAA:4AV7PlSDLxVc7NkeV0hvhPk0qJFgVgo0NrejBL7VLzYer8fpctmlt2uGLtyVZsclpbeG_U-imEi6) doi: 10.1016/J.EPSR.2020.106927
- 942 Reyes, P. I., Pinto, V. A., & Moya, P. S. (2021, sep). Geomagnetic Storm Occur-  
 943 rence and Their Relation With Solar Cycle Phases. *Space Weather*, 19(9),  
 944 e2021SW002766. Retrieved from <https://onlinelibrary.wiley.com/doi/10.1029/2021SW002766> doi: 10.1029/2021SW002766
- 946 Rodger, C. J., Mac Manus, D. H., Dalzell, M., Thomson, A. W. P., Clarke, E.,  
 947 Petersen, T., ... Divett, T. (2017, nov). Long-Term Geomagnetically In-  
 948 duced Current Observations From New Zealand: Peak Current Estimates  
 949 for Extreme Geomagnetic Storms. *Space Weather*, 15(11), 1447–1460.  
 950 Retrieved from <http://doi.wiley.com/10.1002/2017SW001691> doi:  
 951 10.1002/2017SW001691
- 952 Rogers, N. C., Wild, J. A., Eastoe, E. F., Gjerloev, J. W., & Thomson, A. W. P.  
 953 (2020, feb). A global climatological model of extreme geomagnetic field  
 954 fluctuations. *Journal of Space Weather and Space Climate*, 10, 5. Re-  
 955 trieved from <https://www.swsc-journal.org/10.1051/swsc/2020008> doi:  
 956 10.1051/swsc/2020008
- 957 Shinbori, A., Tsuji, Y., Kikuchi, T., Araki, T., Ikeda, A., Uozumi, T., ... Yumoto,  
 958 K. (2012). Magnetic local time and latitude dependence of amplitude of the  
 959 main impulse (MI) of geomagnetic sudden commencements and its seasonal  
 960 variation. *Journal of Geophysical Research: Space Physics*, 117(8), 8322.  
 961 Retrieved from <http://cdaweb.gsfc>. doi: 10.1029/2012JA018006
- 962 Shore, R. M., Freeman, M. P., Coxon, J. C., Thomas, E. G., Gjerloev, J. W.,  
 963 & Olsen, N. (2019, jul). Spatial Variation in the Responses of the Sur-  
 964 face External and Induced Magnetic Field to the Solar Wind. *Journal of*  
 965 *Geophysical Research: Space Physics*, 124(7), 6195–6211. Retrieved from  
 966 <https://onlinelibrary.wiley.com/doi/10.1029/2019JA026543> doi:  
 967 10.1029/2019JA026543
- 968 Shore, R. M., Freeman, M. P., & Gjerloev, J. W. (2017, dec). An empirical or-  
 969 thogonal function reanalysis of the northern polar external and induced mag-  
 970 netic field during solar cycle 23. *Journal of Geophysical Research: Space*  
 971 *Physics*. Retrieved from <http://doi.wiley.com/10.1002/2017JA024420> doi:  
 972 10.1002/2017JA024420
- 973 Shprits, Y. Y., Vasile, R., & Zhelavskaya, I. S. (2019, aug). Nowcasting and  
 974 Predicting the  $\sum K_p/\sum p_i/i_i$  Index Using Historical Values and Real-  
 975 Time Observations. *Space Weather*, 17(8), 1219–1229. Retrieved from  
 976 <https://onlinelibrary.wiley.com/doi/abs/10.1029/2018SW002141> doi:  
 977 10.1029/2018SW002141
- 978 Smith, A. W., Forsyth, C., Rae, I. J., Garton, T. M., Bloch, T., Jackman, C. M.,  
 979 & Bakrania, M. (2021, aug). Forecasting the Probability of Large  
 980 Rates of Change of the Geomagnetic Field in the UK: Timescales, Hori-  
 981 zons and Thresholds. *Space Weather*, e2021SW002788. Retrieved from  
 982 <https://onlinelibrary.wiley.com/doi/10.1029/2021SW002788> doi:  
 983 10.1029/2021SW002788
- 984 Smith, A. W., Forsyth, C., Rae, J., Rodger, C. J., & Freeman, M. P. (2021,  
 985 jun). The Impact of Sudden Commencements on Ground Magnetic Field  
 986 Variability: Immediate and Delayed Consequences. *Space Weather*, 19(7),  
 987 e2021SW002764. Retrieved from <https://onlinelibrary.wiley.com/doi/10.1029/2021SW002764> doi: 10.1029/2021SW002764
- 988 Smith, A. W., Freeman, M. P., Rae, I. J., & Forsyth, C. (2019, nov). The Influence  
 989 of Sudden Commencements on the Rate of Change of the Surface Horizon-  
 990  
 991

- 992 tal Magnetic Field in the United Kingdom. *Space Weather*, 2019SW002281.  
 993 Retrieved from [https://onlinelibrary.wiley.com/doi/abs/10.1029/](https://onlinelibrary.wiley.com/doi/abs/10.1029/2019SW002281)  
 994 [2019SW002281](https://onlinelibrary.wiley.com/doi/abs/10.1029/2019SW002281) doi: 10.1029/2019SW002281
- 995 Smith, A. W., Rae, I. J., Forsyth, C., Oliveira, D. M., Freeman, M. P., & Jackson,  
 996 D. R. (2020, nov). Probabilistic Forecasts of Storm Sudden Commence-  
 997 ments From Interplanetary Shocks Using Machine Learning. *Space Weather*,  
 998 *18*(11). Retrieved from [https://onlinelibrary.wiley.com/doi/10.1029/](https://onlinelibrary.wiley.com/doi/10.1029/2020SW002603)  
 999 [2020SW002603](https://onlinelibrary.wiley.com/doi/10.1029/2020SW002603) doi: 10.1029/2020SW002603
- 1000 Smith, C., L'Heureux, J., Ness, N., Acuña, M., Burlaga, L., & Scheifele, J. (1998).  
 1001 The ACE Magnetic Fields Experiment. *Space Science Reviews*, *86*(1/4), 613–  
 1002 632. Retrieved from <http://link.springer.com/10.1023/A:1005092216668>  
 1003 doi: 10.1023/A:1005092216668
- 1004 Stone, E., Frandsen, A., Mewaldt, R., Christian, E., Margolies, D., Ormes, J., &  
 1005 Snow, F. (1998). The Advanced Composition Explorer. *Space Science Re-*  
 1006 *views*, *86*(1/4), 1–22. Retrieved from [http://link.springer.com/10.1023/](http://link.springer.com/10.1023/A:1005082526237)  
 1007 [A:1005082526237](http://link.springer.com/10.1023/A:1005082526237) doi: 10.1023/A:1005082526237
- 1008 Tan, Y., Hu, Q., Wang, Z., & Zhong, Q. (2018, apr). Geomagnetic Index  
 1009  $K_p$  Forecasting With LSTM. *Space Weather*, *16*(4), 406–416. Re-  
 1010 trieved from <http://doi.wiley.com/10.1002/2017SW001764> doi:  
 1011 [10.1002/2017SW001764](http://doi.wiley.com/10.1002/2017SW001764)
- 1012 Tasistro-Hart, A., Grayver, A., & Kuvshinov, A. (2021, dec). Probabilistic Geomag-  
 1013 netic Storm Forecasting via Deep Learning. *Journal of Geophysical Research:*  
 1014 *Space Physics*, *126*(1). Retrieved from [https://onlinelibrary.wiley.com/](https://onlinelibrary.wiley.com/doi/10.1029/2020JA028228)  
 1015 [doi/10.1029/2020JA028228](https://onlinelibrary.wiley.com/doi/10.1029/2020JA028228) doi: 10.1029/2020JA028228
- 1016 Thomson, A. W., Dawson, E. B., & Reay, S. J. (2011, oct). Quantifying extreme be-  
 1017 havior in geomagnetic activity. *Space Weather*, *9*(10). Retrieved from [http://](http://doi.wiley.com/10.1029/2011SW000696)  
 1018 [doi.wiley.com/10.1029/2011SW000696](http://doi.wiley.com/10.1029/2011SW000696) doi: 10.1029/2011SW000696
- 1019 Tóth, G., Meng, X., Gombosi, T. I., & Rastätter, L. (2014, jan). Predicting the time  
 1020 derivative of local magnetic perturbations. *Journal of Geophysical Research:*  
 1021 *Space Physics*, *119*(1), 310–321. Retrieved from [http://doi.wiley.com/10](http://doi.wiley.com/10.1002/2013JA019456)  
 1022 [.1002/2013JA019456](http://doi.wiley.com/10.1002/2013JA019456) doi: 10.1002/2013JA019456
- 1023 Tsurutani, B. T., & Hajra, R. (2021, mar). The Interplanetary and Magnetospheric  
 1024 causes of Geomagnetically Induced Currents (GICs)  $\geq 10$  A in the Mäntsälä  
 1025 Finland Pipeline: 1999 through 2019. *Journal of Space Weather and Space*  
 1026 *Climate*, *11*, 23. Retrieved from [https://www.swsc-journal.org/10.1051/](https://www.swsc-journal.org/10.1051/swsc/2021001)  
 1027 [swsc/2021001](https://www.swsc-journal.org/10.1051/swsc/2021001) doi: 10.1051/swsc/2021001
- 1028 Turnbull, K. L., Wild, J. A., Honary, F., Thomson, A. W. P., & McKay, A. J. (2009,  
 1029 sep). Characteristics of variations in the ground magnetic field during sub-  
 1030 storms at mid latitudes. *Annales Geophysicae*, *27*(9), 3421–3428. Retrieved  
 1031 from <https://angeo.copernicus.org/articles/27/3421/2009/> doi:  
 1032 [10.5194/angeo-27-3421-2009](https://angeo.copernicus.org/articles/27/3421/2009/)
- 1033 Upendran, V., Tigas, P., Ferdousi, B., Bloch, T., Cheung, M. C. M., Ganju, S.,  
 1034 ... Gal, Y. (2022, may). Global geomagnetic perturbation forecasting  
 1035 using Deep Learning. *Space Weather*, e2022SW003045. Retrieved from  
 1036 <https://onlinelibrary.wiley.com/doi/10.1029/2022SW003045> doi:  
 1037 [10.1029/2022SW003045](https://onlinelibrary.wiley.com/doi/10.1029/2022SW003045)
- 1038 Van Der Walt, S., Colbert, S. C., & Varoquaux, G. (2011, mar). The NumPy array:  
 1039 A structure for efficient numerical computation. *Computing in Science and*  
 1040 *Engineering*, *13*(2), 22–30. Retrieved from [http://ieeexplore.ieee.org/](http://ieeexplore.ieee.org/document/5725236/)  
 1041 [document/5725236/](http://ieeexplore.ieee.org/document/5725236/) doi: 10.1109/MCSE.2011.37
- 1042 Vennerstrom, S., Lefevre, L., Dumbović, M., Crosby, N., Malandraki, O., Patsou, I.,  
 1043 ... Moretto, T. (2016, may). Extreme Geomagnetic Storms – 1868–2010. *So-*  
 1044 *lar Physics*, *291*(5), 1447–1481. Retrieved from [http://link.springer.com/](http://link.springer.com/10.1007/s11207-016-0897-y)  
 1045 [10.1007/s11207-016-0897-y](http://link.springer.com/10.1007/s11207-016-0897-y) doi: 10.1007/s11207-016-0897-y
- 1046 Viljanen, A., Koistinen, A., Pajunpää, K., Pirjola, R., Posio, P., & Pulkki-

- 1047 nen, A. (2010). Recordings of geomagnetically induced currents in the  
 1048 Finnish natural gas pipeline – summary of an 11-year period. *Geophys-*  
 1049 *ica*, *46*(1-2), 59–67. Retrieved from [https://www.geophysica.fi/pdf/](https://www.geophysica.fi/pdf/geophysica_2010_46_1-2_059_viljanen.pdf)  
 1050 [geophysica\\_2010\\_46\\_1-2\\_059\\_viljanen.pdf](https://www.geophysica.fi/pdf/geophysica_2010_46_1-2_059_viljanen.pdf)
- 1051 Viljanen, A., Tanskanen, E. I., & Pulkkinen, A. (2006, mar). Relation be-  
 1052 tween substorm characteristics and rapid temporal variations of the ground  
 1053 magnetic field. *Annales Geophysicae*, *24*(2), 725–733. Retrieved from  
 1054 <https://angeo.copernicus.org/articles/24/725/2006/> doi: 10.5194/  
 1055 [angeo-24-725-2006](https://angeo.copernicus.org/articles/24/725/2006/)
- 1056 Virtanen, P., Gommers, R., Oliphant, T. E., Haberland, M., Reddy, T., Courn-  
 1057 peau, D., ... Contributors, S. . . (2020). SciPy 1.0: Fundamental Algorithms  
 1058 for Scientific Computing in Python. *Nature Methods*, *17*, 261–272. doi:  
 1059 <https://doi.org/10.1038/s41592-019-0686-2>
- 1060 Weigel, R. S., Vassiliadis, D., & Klimas, A. J. (2002, oct). Coupling of the solar  
 1061 wind to temporal fluctuations in ground magnetic fields. *Geophysical Research*  
 1062 *Letters*, *29*(19), 21–1–21–4. Retrieved from [http://doi.wiley.com/10.1029/](http://doi.wiley.com/10.1029/2002GL014740)  
 1063 [2002GL014740](http://doi.wiley.com/10.1029/2002GL014740) doi: 10.1029/2002GL014740
- 1064 Weimer, D. R. (2013, mar). An empirical model of ground-level geomagnetic pertur-  
 1065 bations. *Space Weather*, *11*(3), 107–120. Retrieved from [http://doi.wiley](http://doi.wiley.com/10.1002/swe.20030)  
 1066 [.com/10.1002/swe.20030](http://doi.wiley.com/10.1002/swe.20030) doi: 10.1002/swe.20030
- 1067 Weimer, D. R., & King, J. H. (2008, jan). Improved calculations of interplanetary  
 1068 magnetic field phase front angles and propagation time delays. *Journal of Geo-*  
 1069 *physical Research: Space Physics*, *113*(A1), n/a–n/a. Retrieved from [http://](http://doi.wiley.com/10.1029/2007JA012452)  
 1070 [doi.wiley.com/10.1029/2007JA012452](http://doi.wiley.com/10.1029/2007JA012452) doi: 10.1029/2007JA012452
- 1071 Welling, D. (2019, sep). Magnetohydrodynamic models of B and their use in GIC  
 1072 estimates. In *Geomagnetically induced currents from the sun to the power grid*  
 1073 (pp. 43–65). American Geophysical Union (AGU). Retrieved from [https://](https://onlinelibrary.wiley.com/doi/10.1002/9781119434412.ch3)  
 1074 [onlinelibrary.wiley.com/doi/10.1002/9781119434412.ch3](https://onlinelibrary.wiley.com/doi/10.1002/9781119434412.ch3) doi: 10.1002/  
 1075 [9781119434412.ch3](https://onlinelibrary.wiley.com/doi/10.1002/9781119434412.ch3)
- 1076 Wik, M., Pirjola, R., Lundstedt, H., Viljanen, A., Wintoft, P., & Pulkkinen,  
 1077 A. (2009, apr). Space weather events in July 1982 and October 2003  
 1078 and the effects of geomagnetically induced currents on Swedish techni-  
 1079 cal systems. *Annales Geophysicae*, *27*(4), 1775–1787. Retrieved from  
 1080 <https://angeo.copernicus.org/articles/27/1775/2009/> doi: 10.5194/  
 1081 [angeo-27-1775-2009](https://angeo.copernicus.org/articles/27/1775/2009/)
- 1082 Wing, S., Johnson, J. R., Jen, J., Meng, C. I., Sibeck, D. G., Bechtold, K., ... Taka-  
 1083 hashi, K. (2005, apr). Kp forecast models. *Journal of Geophysical Research:*  
 1084 *Space Physics*, *110*(A4). Retrieved from [http://doi.wiley.com/10.1029/](http://doi.wiley.com/10.1029/2004JA010500)  
 1085 [2004JA010500](http://doi.wiley.com/10.1029/2004JA010500) doi: 10.1029/2004JA010500
- 1086 Wintoft, P., Viljanen, A., & Wik, M. (2016, may). Extreme value analy-  
 1087 sis of the time derivative of the horizontal magnetic field and computed  
 1088 electric field. *Annales Geophysicae*, *34*(4), 485–491. Retrieved from  
 1089 <https://angeo.copernicus.org/articles/34/485/2016/> doi: 10.5194/  
 1090 [angeo-34-485-2016](https://angeo.copernicus.org/articles/34/485/2016/)
- 1091 Wintoft, P., Wik, M., Matzka, J., & Shprits, Y. (2017, nov). Forecasting  $\partial_t Kp_i / i_i$   
 1092 from solar wind data: input parameter study using 3-hour averages and 3-hour  
 1093 range values. *Journal of Space Weather and Space Climate*, *7*, A29. Re-  
 1094 trieved from <http://www.swsc-journal.org/10.1051/swsc/2017027> doi:  
 1095 [10.1051/swsc/2017027](http://www.swsc-journal.org/10.1051/swsc/2017027)
- 1096 Wintoft, P., Wik, M., & Viljanen, A. (2015, mar). Solar wind driven empirical  
 1097 forecast models of the time derivative of the ground magnetic field. *Journal of*  
 1098 *Space Weather and Space Climate*, *5*, A7. Retrieved from [http://www.swsc](http://www.swsc-journal.org/10.1051/swsc/2015008)  
 1099 [-journal.org/10.1051/swsc/2015008](http://www.swsc-journal.org/10.1051/swsc/2015008) doi: 10.1051/swsc/2015008
- 1100 Yue, C., Zong, Q. G., Zhang, H., Wang, Y. F., Yuan, C. J., Pu, Z. Y., ... Wang,  
 1101 C. R. (2010, may). Geomagnetic activity triggered by interplanetary

- 1102 shocks. *Journal of Geophysical Research: Space Physics*, 115(A5), n/a–  
1103 n/a. Retrieved from <http://doi.wiley.com/10.1029/2010JA015356> doi:  
1104 10.1029/2010JA015356
- 1105 Zhelavskaya, I. S., Vasile, R., Shprits, Y. Y., Stolle, C., & Matzka, J. (2019). Sys-  
1106 tematic Analysis of Machine Learning and Feature Selection Techniques for  
1107 Prediction of the Kp Index. *Space Weather*, 17(10), 1461–1486. Retrieved from  
1108 <https://doi.org/10.1029/2019SW002271> doi: 10.1029/2019SW002271
- 1109 Zong, Q.-G., Yue, C., & Fu, S.-Y. (2021, mar). Shock Induced Strong Substorms  
1110 and Super Substorms: Preconditions and Associated Oxygen Ion Dynamics.  
1111 *Space Science Reviews*, 217(2), 33. Retrieved from [http://link.springer](http://link.springer.com/10.1007/s11214-021-00806-x)  
1112 [.com/10.1007/s11214-021-00806-x](http://link.springer.com/10.1007/s11214-021-00806-x) doi: 10.1007/s11214-021-00806-x
- 1113 Zwickl, R., Doggett, K., Sahm, S., Barrett, W., Grubb, R., Detman, T., ...  
1114 Maruyama, T. (1998). The NOAA Real-Time Solar-Wind (RTSW) System  
1115 using ACE Data. *Space Science Reviews* 1998 86:1, 86(1), 633–648. Retrieved  
1116 from <https://link.springer.com/article/10.1023/A:1005044300738> doi:  
1117 10.1023/A:1005044300738